THE CHARACTERISTICS OF DC ARCS AS RELATED TO ELECTRICAL DISCHARGE MACHINING

by

Ronald John Weetman

B.S.M.E., Lowell Technological Institute
(1966)

Submitted in Partial Fulfillment

of the Requirements for the

Degree of Master of

Science

at the

Massachusetts Institute of

Technology

January 1968

Signature of Author . . . . . .
Department of Mechanical Engineering, January 15, 1968

Certified by . . . . . .
Thesis Supervisor

Accepted by . . . . . .
Chairman, Departmental Committee
on Graduate Students

THE CHARACTERISTICS OF DC ARCS AS RELATED TO ELECTRICAL DISCHARGE MACHINING

by

Ronald John Weetman

Submitted to the Department of Mechanical Engineering on January 15, 1968, in partial fulfillment of the requirements for the degree of Master of Science.

ABSTRACT

The purpose of this investigation was to determine the erosion mechanism of electrical discharge machining (EDM). In the EDM process, repeated electrical discharges erode small craters in the workpiece, forming a cavity of the shape of the tool. Because the electrical discharge occurs between the tool and the workpiece, detrimental erosion of the tool also occurs. The main goal of this investigation was to determine the mechanisms governing the relative amounts of erosion occurring at the tool and at the workpiece.

Since it was thought that the only way to understand fully the mechanism of erosion was to relate it to the characteristics of the electrical discharge occurring in EDM, a general study of electrical discharges was undertaken first. It was determined that the characteristics of the EDM discharge were similar to those of a high pressure (1 atmosphere) arc discharge in air. An energy balance analysis at the electrodes (tool and workpiece) was done to determine what percentage of the arc energy is imparted to each electrode. It was shown that $\sim$ 70% of the total arc energy goes to the anode, while only $\sim$ 7% goes to the cathode. A straightforward calculation proves that only 5% of the total arc power is needed to melt the observed amount of eroded metal. The rest of the arc power may qualitatively be accounted for by the power associated with vaporization and incomplete removal of molten metal.

Because the steady state of a carbon cathode arc produces a very low energy density, it was determined that a carbon cathode arc could not cause significant electrode erosion for the arc durations encountered in EDM. Thus it was concluded that most of the erosion was caused by the initiation of the arc, that is, the spark. This spark erosion with a carbon cathode is contrasted to the long duration arc erosion obtained with a low melting point cathode.

Under extreme conditions of large gap distances (0.005" to 0.007") used in EDM, the energy balance analysis prediction of ten times as much erosion occurring at the anode as occurring at the cathode is contradicted by observations of more cathode erosion than anode erosion. This disagreement was reconciled by the observation that the anode is plated by cathode metal. Thus, the plating protects the anode.

It was determined that gas jets emanating from around the cathode spot can propel cathode metal, in its vapor and molten state, to the anode. These gas jets are described by Maecker as resulting from the arc's magnetic field. Thus it was proposed that gas jets are a possible means by which plating is accomplished.

All of the conclusions stated are consistent with experiments done with a single discharge apparatus and an Elox EDM machine; however, these conclusions cannot be said to have been experimentally proven because the number of tests that have been run is limited.

Thesis Supervisor: Robert E. Stickney
Title: Associate Professor of Mechanical Engineering

ACKNOWLEDGMENTS

The author wishes to thank Professor Robert E. Stickney for his help and guidance throughout this investigation. Also, appreciation is extended to Ernest DeNigris, a fellow student, for his discussions on EDM and to Stanley Doret, Hans C. Juvkam-Wold, and T. Viswanathan, other fellow students, for sharing the results of their experimental work in EDM. Gratitude is expressed to Professor Sanborn Brown for his help in understanding the properties of arcs. Recognition is given to Miss Lucille Blake for her expert typing of this thesis.

Thanks are offered to the Elox Corporation of Michigan for their financial support during the first year of this investigation and to the Mechanical Engineering Department of M.I.T. for its monetary aid in the last five months of this project.

Special appreciation is given to my wife, Joan, for her patience and encouragement.

TABLE OF CONTENTS

LIST OF FIGURES

1.0 INTRODUCTION

Electrical discharge machining (EDM) is a relatively new process of machining with a pulsed DC arc. Arc discharges occurring at a frequency of from 0.2 KC to 250 KC are used to erode the surface of the workpiece to be machined. Since each discharge erodes a small crater in the workpiece, repeated discharges erode (or machine) the workpiece in the shape of the tool. With the arc taking place between the tool and workpiece, erosion also occurs on the tool. This means that the most important factor in improving EDM is to reduce the erosion of the tool while maximizing the erosion or machining of the workpiece.

A good description of the work that has been done in EDM has been given by Berghausen, Brettschneider, and Davis[1] and by Barash[2]. Although a considerable amount of work has been done in studying the EDM process, the actual mechanism that causes erosion of the electrodes (tool and workpiece) is not very well understood. It is easy to see why the EDM erosion mechanism is not understood since the mechanism of an arc discharge has not been fully established. In fact there are many contradicting theories that have been put forth to explain the mechanism of the arc discharge.

Most of the work done in studying EDM has been empirical in nature. In the majority of cases, the work merely describes the bulk quantities, such as the total erosion of the electrodes after repeated discharges. Because of this lack of detailed data on the arc discharge in the EDM literature, this thesis will describe the characteristics of arcs as they are related to EDM.

The characteristics of arcs will be presented first, and then these will be compared to the properties encountered in EDM. After these arc characteristics, which are studied from the physicist's viewpoint, are related to the EDM process, they will be used to determine the energy balances at the electrodes.

In the use of EDM there seem to be certain conditions when the analysis of electrode erosion using the energy balances fails. This failure seems to occur when high energy pulses and large gap distances between the electrodes are used. Unfortunately these two conditions have not been independently established since the large gap distances are dependent upon the energy discharged per pulse in the EDM machines currently used. This dependence is accomplished by the large energy pulses eroding large particles which in turn makes the arc breakdown at large gap distances.

The apparent reduction of anode erosion is the effect that cannot be explained using the energy balance analysis. Under extreme conditions of very large energy pulses and gap distances, a build-up of cathode material on the anode is found. In an effort to explain this depositing or plating of cathode material on the anode, an analysis is given of gas and erosion jets that emanate from the regions around the electrodes.

2.0 CHARACTERISTIC OF ARCS

Because of the lack of satisfactory experiments and theories on the exact nature of the electrical discharge occurring under EDM conditions, a study of the existing literature on arcs was undertaken. The following chapter presents the characteristics of arcs found in the literature and compares these with the properties of the discharge occurring in EDM. The properties of the EDM discharge are found in the literature on EDM and from experiments done by Stanley A. Doret[3], Hans C. Juvkam-Wold[4,5], and T. Viswanathan[4,6] here at M.I.T. The experiments by Stanley A. Doret were done on a single-discharge apparatus which enabled us to analyze the properties of a single discharge. Properties of continuous EDM were obtained by Hans C. Juvkam-Wold and T. Viswanathan on an Elox EDM machine.

All of the references on the characteristics of arcs (unless stated otherwise) use arcs in air, at atmospheric pressure, in their experiments. Although the arc discharge occurring in EDM is in a liquid dielectric (usually oil), we want to show that the arc discharge in air and in oil are alike by showing that their characteristics are similar. By showing this similarity we can use the characteristics and theories developed for arcs in air in analyzing the EDM process.

2.1 Definition of Sparks and Arcs

Since the terms spark and arc are sometimes used interchangeably, we shall take the generally accepted definition of each and use these throughout the discussion. Referring to Fig. 1, a plot of the different discharges that can occur between two electrodes (see Appendix C),

the arc region is characterized by low voltages (<50 volts) and high currents (>3 amps). The plot is for varying the current across a gap of about a few centimeters. But if the voltage is suddenly applied to a gap and the circuit allows the current to be >3 amps, the curve would show a discontinuous jump from F to G instead of the smooth transition to H. This sudden occurrence of an arc can be seen on Fig. 2 as a function of time. The non-steady region of the plot (time $<10^{-6}$ sec) is called a spark discharge which leads into the quasi-steady state called the arc. Quasi-steady is used because it is not in complete thermal equilibrium with its surroundings.

Somerville, Blevin, and Fletcher[7] indicate this quasi-steady characteristic when they analyze the apparent decrease in current density with time. They say that this decrease in current density, or actually the increase in the size of the crater left on the electrode, is from heat conduction in the case of the anode and from motion of the emitting areas in the case of the cathode.

The term arc, which will be of duration t (1 μ sec < t < 1 m sec), will be used to describe the discharge process for electrical discharge machining in this paper. This should not be confused with the term arcing used in electrical discharge machining literature as a failure. This arcing is from a short circuit, formed by a high density of metallic vapors from the electrodes, which does not shut off when the voltage is shut off (in one cycle). This results in a large pit in the work piece.

2.2 Properties of Arcs

The following properties of arcs are put forth to enable us to better understand arcs in general and especially the electrical discharge that occurs in EDM. After presenting the properties of arcs, in air at atmospheric pressure, we shall compare these with the properties that we have encountered in EDM.

2.2.1 Electrode Fall Potentials

Some of the properties of an arc can be seen in Fig. 3. Part a of Fig. 3 shows the profile of the discharge denoting its three regions. A net space charge of positive ions is built up in the cathode fall region accelerating the ions toward the cathode. At the anode a space charge of electrons (anode fall) is set up which in turn accelerates the electrons to the anode. The potential across the gap shown in part b of Fig. 3 illustrates the sharp rise in potential in the electrode fall regions. The cathode fall potential is generally about 10 volts[8] for refractory (C,W) and low melting point metals (Cu, Fe), but the anode fall potential is usually different for these two classes of metals. Blevin[9] gives the value of the anode fall potential for low melting point metals as ranging from 2 to 9 volts. These values agree with Somerville's[10] values of 1 to 12 volts, which increase with decreasing current. These are substantiated by values given by Von Engel[11], but Somerville's values for the anode fall potential for carbon cathodes (25 to 35 volts) differ from Von Engel's values of 11-12 volts. Since Somerville states that the anode fall potential decreases from 35 volts to 25 volts for increasing current, we believe that these figures could be in agreement with Von Engel's at a high enough current.

Because of the high currents used in EDM, we shall use the values of 11 to 12 volts for the anode fall potential with carbon electrodes. These low values for the anode fall potential for refractory metals (C,W) at high currents are supported by Busz-Peuckert and Finkelnburg's[12,13] measurements for the anode fall potential for tungsten. Busz et al. also showed that the anode fall potential for tungsten increased somewhat with gap distance. For gap distances between 2 and 10 mm., they found the anode fall potential increasing from 8 to 12 volts for a 20-amp arc.

2.2.1.1 Arc Discharge Potential in EDM

The arc potentials measured on the single-discharge apparatus agree quite well with the predicted values above. In comparing the arc potentials observed in EDM, the total arc potential will be assumed to be the sum of the cathode and anode falls. The justification for neglecting the plasma potential will be discussed in Section 2.2.4. Summing the electrode falls from the previous section, it is expected that the arc potential using low melting point electrodes would range from 12 to 19 volts, and the arc potential using refractory electrodes would range from 20 to 21 volts. The arc potentials observed on the single-discharge apparatus were 11 to 16 volts for low melting point electrodes, and 19 volts for carbon electrodes. These observed values agree quite well with the expected values, especially illustrating the low anode falls in low melting point metals as compared to the higher value for refractory electrodes. In the limited number of tests run, the arc potential for low melting point electrodes seems to increase somewhat with increasing gap spacing. This could be similar to the observations of Busz et al.[12,13] where the anode fall increased with increasing gap distances.

2.2.1.2 Physical Significance of Electrode Falls

The physical significance of the electrode falls is seen in the following chapter where they will then be used in the energy balance analysis. Because the cathode fall accelerates the ions, additional energy is given to them. When these ions impinge upon the cathode, this additional energy is imparted to the cathode. The anode fall likewise increases the energy of the electrons. This increased energy is also transformed into thermal energy as the electrons impinge upon the anode. The liberated energy at the electrodes will be accounted for in terms of the erosion of the electrodes in the following chapter.

The effect of the electrode falls on impinging particles as stated above is actually a by-product of the original purpose of the electrode falls. The purpose of the electrode falls is to supply a transition region between the metal conductors (i.e., electrodes) and the plasma column. Thus, the cathode fall accelerates the electrons emitted from the cathode until they have sufficient energy to ionize the gas between the electrodes to form a plasma. In a similar manner, the anode fall supplies a transition region for ion current being present in the plasma to only the electron current existing in the anode.

2.2.2 Current Densities

The current densities at the electrodes are the most important factors in determining the energy density to the electrodes. Unfortunately the measurement of the current density (or more correctly the area, since the total current is easily obtained) at the electrodes is a difficult measurement to make. The difficulty arises because of the

large constriction from the plasma column to the electrode surface in the distance of a few electron mean free paths. This means that the electrode surface is obscured by the luminous plasma close to the surface.

Another problem that has misled many investigators in determining the cathode current density is the erratic motion of the arc over the cathode surface. If the current density were determined by photographing the arc over a large time interval (time > 1 m sec), this motion of the arc over the cathode surface would give a much lower current density than its true value. This same motion would also give an apparent low current density for the following reason. If the current density were calculated using the area of the mark or crater formed by a long duration arc on the cathode surface, a low current density would result.

These two problems mentioned above have been overcome by Froome[14,15,16] with the use of a 1 μ sec exposure Kerr cell shutter. With this fast exposure time, Froome can arrest the arc's erratic motion over the cathode surface. Another method that gives fairly good results in measuring the current density is to measure the track left by the arc after the arc has been swept across the electrode surfaces by a magnetic field. This method was employed by Cobine and Gallagher[17] to show that the previously determined values (Druyvestyn and Penning[18]) for the cathode current densities of low melting point metals were too low. Cobine and Gallagher obtained cathode current densities ranging from 10^4 to 10^6 a/cm^2 for low melting point metals (Fe Cu).

Another misconception that Froome corrects is the belief by some investigators that the current density decreases with the duration of the arc. Froome[15] describes the cathode spot as follows:

"The bright, erratically moving spot which one sees upon the cathode is actually a relatively slow-moving envelope containing several minute emitting areas each carrying a current of the order of 1 amp. When the arc current exceeds 5-30 amp, two or more such groups are formed and so on for increasing currents. These tiny areas are much faster moving than their containing envelope, and microsecond exposures through a microscope are needed to arrest their motion and reveal their minuteness. The apparent size of these areas is quite independent of the time from the start of the arc, being observed the same for transient arcs of a few microseconds duration or for normal DC arcs one-two-hundredth of a second after the start."

Froome believes that the current densities of low melting point metals always exceed 10^6 a/cm^2.

The cathode current density is the sum of the ion and electron current density as shown in Fig. 3c. It is generally assumed (Somerville[19]) that the ion current to the cathode represents about 10% of the total current. Although this value of 10% has never been verified experimentally, it does agree with the energy balance calculations at the electrodes.

For refractory metals (C,W) the cathode current density has a transition from low values that could explain thermionic emission (10^2 to 10^3 a/cm^2) to high values (10^5 a/cm^2)[20] similar to low melting point metal cathodes. This transition occurs as the pressure is decreased to below a certain critical pressure, P_c.

Von Engel and Arnold[21] describe this transition for an arc in air between carbon electrodes changing from a thermionic arc to what they call a vapor arc. For a 5-amp arc the critical pressure is ∿100 mm Hg. Below this pressure the arc contracted, and carbon vapor was observed. There was also a decrease in arc voltage of 10 to 30 volts. Von Engel and Arnold also say that P_c decreases with increasing current and with increasing gap distance. Somerville[20] reports on this transition for a tungsten cathode.

The low value of the current density (10^3 a/cm^2) will be calculated from the Dushman equation for thermionic emission. This equation is given by Cobine[22] for carbon in the following form:

$$j = 5.93\ T^2 \exp\left(-\frac{46{,}500}{T}\right) .$$

If Cobine's value for the boiling point of carbon is used (4473 ^{o}K), the current density equals:

$$j = 5.93\ (4473)^2 \exp\left(-\frac{46{,}500}{4473}\right)$$

$$= 3 \times 10^3 \text{ amp/cm}^2 .$$

This value of 3×10^3 a/cm^2 is the maximum value that would be expected at atmospheric pressure.

The current density at the anode is usually an order of magnitude less than the cathode current density. For low melting point metals, it ranges from 10^3 to 10^5 a/cm^2 (Somerville[23], Cobine and Burger[24]). The same transition affects the anode current density at refractory

metals as stated above. Somerville[25] reports that the anode current density of carbon can change from $\sim 10^2$ a/cm^2 to 10^3 a/cm^2 for small spots within the anode termination.

2.2.2.1 Current Densities in EDM

The same problems stated in the previous section were encountered in analyzing the marks or craters formed in EDM. Some of the cathode craters formed using the single-discharge apparatus indicated low current densities (10^3 a/cm^2) for low melting point metals[3]. But fortunately in one of the long discharges, the arc moved from one large crater to another showing the path between them. The photograph in Fig. 4a shows this path which indicates a current density of greater than 10^5 a/cm^2.

Also, Fig. 4b shows a shorter discharge that represents current densities greater than 10^5 a/cm^2.

These values for the current density also agree with values of 10^5 a/cm^2 found by Barash[2] for EDM. Since the crater would represent the envelope mentioned by Froome[15], we could expect the current density to exceed 10^5 a/cm^2.

A surprising result was obtained when examining the anode current density from a carbon cathode. Instead of 10^2 a/cm^2 given in Section 2.2.2, the crater on the anode indicated a current density of 10^5 a/cm^2. Because this crater resulted from an arc at atmospheric pressure, the possibility of it being the vapor arc described by Von Engel and Arnold[21] is ruled out.

The cause of this high current density was determined to be the initiation process (spark) of the arc. This was accomplished by

examining craters formed on the anode in arcs ranging in duration from 13 μ sec. to 3200 μ sec. This analysis showed that the craters formed were about the same diameter and depth, indicating that they were made in times less than 13 μ sec. Since our lower limit for arc duration was 13 μ sec. on our single-discharge apparatus, we could not reach the expected spark duration of 1 μ sec. Even though we did not reach 1 μ sec., we believe that the crater formed on the anode from a carbon cathode is from the spark. It is not until after a few seconds that melting caused by the arc is noticed.

See Appendix B for more details on the refractory spark.

2.2.3 Constrictions at Electrodes

The following two theories will be used to explain the constriction of the arc column at the anode (see Fig. 3a). Although there is no generally accepted theory of why the arc constricts at the anode, these two theories both use the radial temperature in their hypotheses.

Somerville[26] describes Bez and Hocker's[27] theory of the anode constriction caused by two distinct types of ionization mechanisms in the anode fall region. Bez and Hocker state that field ionization, which is ionization by electrons traveling through a high electric field, occurs at the periphery of the arc. The other type of ionization is thermal ionization which Bez and Hocker say will be present at the hot center of the arc. The important differences between field and thermal ionization are the following: Field ionization occurs over a distance of about one electron mean free path, whereas thermal ionization takes place over several mean free paths. Also, the potential needed for field ionization is greater than the potential in thermal ionization.

The consequent distribution of potential over the arc will tend to drive electrons toward the center and therefore constrict the arc.

The second theory used to explain the anode constriction is by Von Engel[28]. With the temperature and current density greatest at the center of the arc, Von Engel says that intense evaporation will occur at the center. Since the metallic vapor is usually more readily ionized than a gas, ionization will be favored nearer the axis, and as a result of this, the positive column constricts.

With the many theories proposed for the emission of electrons from the cathode (to be discussed in Section 2.3 below), it can be expected that the cause of the constriction at the cathode is not known with any degree of certainty. Two qualitative theories put forth by Elenbaas[29] also depend upon the radial temperature distribution across the arc as did the previous theories for the anode constriction. Elenbaas suggested that if thermionic emission is the electron emission mechanism, then emission might only occur at the hot center of the arc. Elenbaas used the following description for the cause of the constriction when field emission is the emission mechanism. Since the center of the arc is the hottest, it will have the greatest ionization; therefore, the electric field will be strongest at the center. Thus emission will tend to be greatest at the center of the arc, hence causing a constriction.

Another approach to explain the constriction at the cathode is to consider the radial diffusion of the electrons after they have been emitted from the cathode. This radial diffusion will proceed across

the cathode fall until the velocities of the electrons become randomized to form a homogeneous plasma upon ionization in the column. Llewellyn Jones[30] derives an expression for radial electron diffusion in the presence of ions. Although he uses this expression to explain the electron avalanche phenomenom for the initiation of a spark, it could be used to describe the constriction at the cathode.

2.2.3.1 Profile of EDM Arc

The profile of the EDM arc can be analyzed from Fig. 3a if the plasma column is essentially eliminated. The result of this elimination of the column is seen in Fig. 5. Although the plasma column is actually still present, the expansion of the luminous gas gives the appearance of only the cathode fall region.

2.2.4 Longitudinal Electric Field in the Plasma Column

In order to determine if the potential along the plasma column contributes significantly to the total arc potential in the short gaps encountered in EDM, the longitudinal electric field in the plasma column is studied. Fig. 6 shows how the electric field, for arcs in air and water vapor, varies with current. Von Engel states that the electric field is larger for water vapor than air because water vapor has larger heat conductivity and dissociation losses, and this necessitates a larger electric field to balance the losses. The electric field also decreases with the current probably because the gas temperature increases with current.

2.2.4.1 Plasma Potential in EDM

With the maximum electric field of 300 v/cm for water vapor at 1 amp that might occur in EDM, the voltage across the plasma would be

about 9 volts for a 0.010-inch (0.025 cm) gap. But this potential across the plasma will drop to 1 volt for a current of 15 amps. Water vapor was used above to analyze the potential across the plasma for EDM since water gives similar results to oil when used as a liquid dielectric in EDM (Berghausen et al.[1]).

2.2.5 Temperature of the Arc

Fig. 7 shows that atpressures greater than 10 mm Hg the electrons have enough collisions with the atoms to make the electron and gas temperatures approximately equal. Somerville[31] states that the gas temperature varies from 5000 ^{o}K to 50,000 ^{o}K prevailing at high pressures. For air at atmospheric pressure Suits[32], using the technique of observing the velocity of sound through the arc, determined the temperature of approximately 6000 ^{o}K. Suits' temperature is in general agreement with other observers using spectroscopic techniques (Somerville[33]).

The radial distribution of temperature in a mercury arc is seen in Fig. 8. This illustrates that the temperature does not fall off to a high degree over the conducting area.

2.2.6 Conducting Profile in the Plasma Column

Elenbaas[34] gives a good description of the profile of the conducting channel of a high pressure arc. By assuming thermal equilibrium, Elenbaas uses the Saha thermal ionization equation to predict the sharp fall of the conducting profile shown in Fig. 8. The Saha equation of the form

$$\frac{n_i n_e}{n_a} = \frac{(2\pi m_e k)^{3/2}}{n^3} 2\left(\frac{g_i}{g_a}\right) T^{3/2} \exp\left(\frac{-eV_i}{kT}\right)$$

where

n_a = number density of atoms

n_i = number density of ions

n_e = number density of electrons

m_e = mass of an electron

g = ground state degeneracies

V_i = ionization potential

can be reduced to

$$n_e \sim T^{1/4} \exp\left(\frac{-eV_i}{2kT}\right) .$$

This proportionality uses the fact that $n_i = n_e$ in the plasma column and that $n_a \sim \frac{1}{T}$ from $P_a = n_a kT$. Elenbaas calculates n_e for mercury with $V_i = 10.43$ volts to be

$$n_e \sim T^{1/4} \exp\left(-\frac{60{,}500}{T}\right) .$$

From the temperature profile in Fig. 8, that can be determined experimentally, Elenbaas selects two temperatures to show the sharp drop in electron number density. He calculates that the electron number density drops by 99.4% as the temperature goes from 6000 ^{o}K to 4000 ^{o}K. Since the current density, $j = e\, n_e v$ and $v \sim T^{1/2}$, the current density at 4000 ^{o}K is less than 0.6% of the current density at 6000 ^{o}K.

The above use of the Saha equation illustrates why the plasma column constricts for high pressure arcs. Von Engel shows this constriction occurring at high pressures in Fig. 9. This constriction occurs because of the increased gas temperature with pressure. At

low pressures the ionization is caused by the electrons bombarding the neutral atoms. Since the electron temperature is almost uniform across the diameter of the tube, the electron density does not fall off as rapidly as it does at high pressures. The electron density falls off at low pressures because of diffusion and recombination, whereas at high pressures the sharp drop in temperature accounts for most of the constriction of the conducting channel.

2.2.7 Short Arcs

The cathode and anode fall are usually of the order of one electron mean free path, λ_e. This is about 10^{-3} to 10^{-4} cm for atmospheric air (Somerville[35]). If the total length of the gap between the cathode and anode is of the order of one electron mean free path, the arc is called a short arc (Llewellyn Jones[36,30]). Llewellyn Jones states that for a short arc the electrons will bombard the anode causing erosion. But if the gap is made longer ($\geq 100\ \lambda_e$), the electrons will have many collisions and therefore lose their energy. The ions will then be accelerated in the cathode fall which will erode the cathode. This arc is called a cathode arc, and the former arc is called an anode arc. In the case of a high-power arc, the longer arc may have more erosion of the anode if an anode fall is established. Germer and Boyle[37] give some data for short arcs although the duration of the arcs is $\leq 1\ \mu$ sec. which presents some problems with multiple spots that will be discussed in Section 2.4 of this chapter. The anode and cathode arcs at a breakdown voltage of 300 volts give an average gap distance of 3×10^{-5} cm and 7×10^{-5} cm, respectively. The breakdown voltage of 300 volts was used because it is needed for cathode arcs,

although anode arcs will occur down to 50 volts. The gap voltages after breakdown are also different being 9-12 volts for anode arcs and 13-18 volts for cathode arcs. This data supports Llewellyn Jones' ideas although Germer and Boyle's explanation of the cathode arc differs from Llewellyn Jones'. Germer and Boyle say that the multiple erosion pits on the cathode are caused by melting of points from the field emission currents flowing through them.

2.2.7.1 Short Arc in Electrical Discharge Hardening

Although the short arc, specifically the anode arc, is not the case observed in EDM, it seems beneficial at this time to mention that the anode arc does correspond to the situation observed in electrical discharge hardening (see Barash and Kahlon[38]). This hardening process is accomplished by using repeated electrical discharges between an anode of hard metal and a cathode of soft metal. A plating of hard anode material is deposited on the cathode during the discharges in an air atmosphere.

We believe that the arcs occurring in the process of hardening are anode arcs because of the following reasons: First, the breakdown voltages employed in the hardening process range from 60 to 110 volts (see Barash and Kahlon[38]), which is the lower range for anode arcs. Another reason to believe that these are anode arcs is that one of the electrodes has to be vibrated in order to prevent welding of the two electrodes together. This welding of the two electrodes is exactly what Germer and Boyle[37] observed for the majority of anode arcs.

One interesting observation which was made by Barash and Kahlon that may apply to EDM is the following: Plating took place at a much

higher rate from metals with a higher melting point on to metals with a lower melting point than vice versa. A possible explanation offered by Barash and Kahlon for this higher rate was that the vapor from the high melting anode could condense on the cathode, and in doing so produce sufficient heat to melt the cathode surface and produce a strong bond.

2.3 Mechanisms of Electron Emission

The mechanism explaining how electrons are emitted from the cathode surface is fundamental to the understanding of the arc discharge. Although many mechanisms for this emission of electrons have been proposed, no theory has been specified in enough detail to be generally accepted. The difficulty that arises in supporting the many proposed theories is the problems encountered in measuring properties in the cathode fall region. Properties (i.e., electron current density, ion current density, etc.) cannot be measured because of the small size of the cathode fall region. The cathode fall region extends over a distance of a few electron mean free paths (Somerville[35]), which is less than 10 μ at atmospheric pressure. Many of the theories that have been proposed will be stated below.

The one theory that explains a limited range of conditions is thermionic emission. This accounts for the low current densities (10^2 a/cm^2) of refractory metals because of their ability to achieve a high enough temperature without evaporating. But it does not explain the high current densities (10^5 a/cm^2) that are encountered in the transition of refractory metals to a vapor arc (Von Engel and Arnold[21]). Thermionic emission also cannot explain the high current density (10^6 a/cm^2) of low melting point metals.

Field emission was formerly thought to be the mechanism for low melting point metals. It could explain 10^3 to 10^4 a/cm^2, thought to be the current density (Druyvestyn and Penning[18], Mackeown[39]). But with the current density now realized to be 10^5 to 10^6 a/cm^2, the field emission mechanism first developed by Langmuir cannot substantially account for these high-current densities (Cobine and Gallagher[17], Somerville[40]).

Another mechanism suggested by Druyvestyn[18] is that of electron emission through insulating layers on the surface resulting from positive ions building up on the insulator. This is also suggested as the mechanism by Cobine and Gallagher as a result of the need to oxidize copper and tungsten before any noticeable erosion was observed. Somerville, Blevin, and Fletcher[7] also had to oxidize Cu and W before any appreciable signs of melting occurred.

Slepian suggested a thermal ionization theory that was later extended by Weizel, Rompe, and Schon and Ecker (Somerville[41]). The theory is that in some high pressure arcs a highly ionized layer of gas or vapor close to the cathode may supply a large fraction of the cathode current in the form of positive ions.

A quite involved theory is developed by Von Engel and Robson[42] which explains that a dense layer of metal atoms vaporized from the electrodes exists in front of the cathode. This layer is caused by momentum transfer from the cathode fall potential. These atoms are put into an excited state and then hit the cathode giving up their excitation potential in removing an electron. These excited atoms can be quenched by the gas molecules by transferring their excitation

potential to the gas molecules. Since molecules have a smaller probability of removing an electron from the cathode, this quenching is used to explain the transition of refractory metals from a high-current density vapor arc to a thermionic arc (Von Engel and Arnold[21]). Von Engel and Robson's theory proposes a vapor pressure of 10 atm. at the cathode, but as yet there is no experimental proof to support these high pressures for a sustained arc (Somerville[43]).

Other attempts have been made to try to explain the high-current densities of low melting point metals and in the vapor arc mode of refractory metals by combining different emission processes. Somerville[44] tells of Bauer's attempt to explain these high current densities by combining thermionic and field emission.

A later paper by Eather[45] explains the high current densities by combining three ideas. Essentially Eather only uses one theory but modifies and supports this with two others. He uses J. Rothstein's theory[46] which states the existence of a dense vapor layer having continuous (including conduction) energy bands next to the cathode. This would allow metallic conduction from the cathode to this vapor, which in turn, being at a very high temperature, would emit electrons by thermionic emission. Eather supported the existence of the dense vapor layer by Von Engel and Robson's[42] theory. In order that Rothstein's theory of thermionic emission account for 10^5 to 10^6 a/cm^2, Eather used A. M. Cassie's[47] theory of lowering the work function of the cathode by the pinch effect. This effect is the inward radial force caused by the self-magnetic field of the arcs.

2.3.1 Importance of Electron Emission Mechanism in EDM

Since the exact mechanism of electron emission has not been resolved yet, we could not hope to determine the electron emission mechanism occurring in EDM. But in the physicist's search for the emission mechanism, he has found that the current density of carbon (or graphite) is only 10^2 to 10^3 a/cm^2 (see Section 2.2.2) for high currents and high pressures. This means that when graphite is used as the cathode in EDM, it will produce very low-current densities as compared to a low melting point metal being used as the cathode.

2.4 Multiplicity of Marks on Electrodes

The multiplicity of electrode marks left on the cathode and anode have been studied by Somerville and Grainger[48,49]. They observed that the anode mark may consist of up to 100 separate pits, but the cathode usually had only one or two pits. Their study showed that the factors which caused multiplicity on the anode was a thin contaminating layer, thickness of 10^{-6} cm being sufficient, and a high initial rate of increase of current (> 10^7 a/sec.). If the arc (or probably more correctly, spark) lasted more than 8 μ sec., the pits started to enlarge and combined to form a single mark.

2.4.1 Advantage of Multiplicity of Marks in EDM

The multiplicity of anode marks may be able to be used to an advantage in electrical discharge machining. If the surface in electrical discharge machining is contaminated, and if it is possible to achieve such high rates of current, it might be able to achieve a better surface finish (by having more pits per discharge) at a higher machining rate.

2.5 Arcs in Air and Liquid

Because the mechanism of electron emission has not been established, the only comparison that can be made between arcs in air and in a liquid is their characteristics.

The first characteristic that was shown to be similar for arcs in air and in a liquid was the arc potential. The low values for the discharge potential indicate an arc discharge rather than some other type of electrical discharge. Also, from the steadiness of the discharge potential (see Fig. 10), a steady arc discharge is indicated as compared to a spark discharge, although Fig. 10 shows us that the arc discharge was probably initiated by a spark discharge.

Another important property that was found to be the same in arcs in air and our EDM arc was the high current densities. A few tests were run in air on the single-discharge apparatus to determine if there were any differences between the arc in air and in a liquid. The voltage potential and current density observed were approximately the same values. The only apparent difference was that the craters formed on the electrodes in a liquid were a little deeper and more well defined than the craters on the electrodes in air. This result, which indicates that the liquid seems to enhance the metal removal rate in EDM, was also observed by Barash[2].

Another indication that the arc in a liquid is similar to an arc in air is the high temperatures observed in arc discharges. In fact, an arc in air with its gas temperature of 6000 ^{o}K will certainly not allow liquid to remain in the arc column. An example of water surrounding an arc is the Gerdien arc (see Somerville[50]). A Gerdien arc has

water flowing around its periphery, and Somerville reports that axial gas temperatures of over 50,000 ^{o}K have been observed in Gerdien arcs.

In Appendix B it is reported that electrode vapor is observed even in nanoseconds arcs. Since some evaporation of the electrodes occurs in high pressure arcs, the arc burns in this vapor given off, as well as the gas initially present between the electrodes. Thus it is proposed that an arc in a liquid will burn in the vapor of the electrodes, as well as the vaporized liquid. This means that an arc in air and in a liquid should be similar if significant electrode evaporation occurs. This importance of electrode vapor is exemplified in vacuum arcs. Since there is no gas present, the vacuum arc burns totally in the vapor from the electrodes. The dependence of electrode vapor in an arc in air can be shown by comparing the cathode fall potentials of arcs in air and arcs in a vacuum. In observations made by Kesaev[51], the cathode fall potentials for an arc in air and in a vacuum were usually within 10% of each other for fourteen different metals. The similarity of these cathode fall potentials indicates that the arc in air is probably burning in vapor from the cathode.

Since it seems that the arc characteristics are the same for arcs in air and in the discharge occurring in a liquid dielectric, these properties will be used in the following chapter in the energy balance analysis. We believe that it has been advantageous to first show that the EDM discharge is similar to a high pressure (1 atmosphere) arc in air for the following reasons: By showing that all of the properties that we have measured are the same, we hope to say that the properties

we cannot measure are the same. Also, if the arcs are similar we may use the proposed theories and descriptions of arcs in air to describe our EDM discharge.

3.0 ENERGY BALANCE AT THE ELECTRODES

In an effort to determine the erosion mechanism in EDM, the following approach to determine the energy flux to the electrodes will be used. This approach is to calculate the energy balance at each electrode and to find out what percentage of the energy dissipated in the arc goes to each electrode. Along with determining these percentages, it is also very important to find out the value of the energy fluxes to the electrodes, since the magnitude of this energy flux will determine if melting and vaporization are possible.

The following formulations of the energy balances at the electrodes are derived from work done by Somerville[52], Finkelnburg[53], and Cobine and Burger[24].

The energy balance at the cathode can be put in the following form:

$$j_c^+ (V_c + V_i + V^+ - \phi) + R_G = j_c^- \phi + M_c + E_c + R_c + C_c \text{ watts/cm}^2$$

where

j_c^+ = ion current density to the cathode — amp/cm^2

V_c = cathode fall — volts

V_i = ionization potential

V^+ = thermal energy of ion

$j_c^+ \phi$ = energy used from extracted electrons to neutralize ions

R_G = radiation from gas

ϕ = work function of cathode

j_c^- = electron current from cathode

M_c = melting of cathode

E_c = evaporation from cathode

R_c = radiation from cathode

C_c = conduction from cathode

Although the above neglects conduction and convection from the gas, they can usually be considered negligible[52]. The equation does include some terms that may also be neglected under certain conditions.

The energy balance at the anode is simpler than that at the cathode. This is because electron emission can be neglected at the anode. The energy balance at the anode is given as follows:

$$j_a^- (V_a + \phi + V^-) + R_G = M_a + E_a + R_a + C_a \qquad \text{watts/cm}^2$$

where

j_a^- = electron current density to the anode amp/cm^2

V_a = anode fall

V^- = thermal energy of electrons

R_G = radiation from gas

M_a = melting of anode

E_a = evaporation from anode

R_a = radiation from anode

C_a = conduction from anode

The energy balance from the anode also neglects conduction and convection from the gas as did the energy balance for the cathode.

3.1 Previous Applications of the Energy Balance at the Electrodes

Before applying the above equations to EDM, several previous applications of the energy balance equations will be shown below.

3.1.1 Finkelnburg

Finkelnburg[53] uses the equation

$$j_c^+ V_c - j_c^+ \phi = j_c^- \phi + E_c$$

for the energy balance at the cathode, therefore neglecting some of the above terms. For the anode he uses $j_a^-(V_a + \phi) = E_a$ for his simplified energy balance. Finkelnburg uses the previous two equations to explain the appearance of vapor from mercury cathodes and generally the absence of vapor from carbon cathodes. He states that since carbon can achieve a high enough temperature for thermionic emission, the energy input to the cathode, $j_c^+V_c - j_c^+\phi$, will be used to emit electrons, $j_c^-\phi$. This would mean that there would not be enough energy remaining for evaporation. Finkelnburg contrasted this with the probable inability of the mercury cathode to have thermionic emission as its mechanism of emission of electrons. Thus the $j_c^-\phi$ term in the cathode energy balance for mercury vanishes, and the energy input can be used for evaporation.

3.1.2 Cobine and Burger

Another paper on the erosion of electrodes is by Cobine and Burger[24] who use the anode energy balance equation as follows:

$$j_a^-(V_a + \phi + V^-) = E_a.$$

With this first-order approximation, all the power is carried off by evaporation. Cobine and Burger compared the evaporation power (watt/cm^2), which is equal to the rate of evaporation ($\frac{\text{gm}}{\text{cm}^2\ \text{sec.}}$) times the latent heat of evaporation (watt/gm), with the range of input powers $[j_a^-(V_a + \phi + V^-)]$ versus temperature. In this comparison they find that the surface temperature of the anode would be greater than its boiling point. The theory is substantiated by data of eroding anodes using very

high currents (11,000 - 26,000 amps peak for a single half cycle, A. C.) assuming that all the erosion was from evaporation.

Cobine and Burger also analyze the energy balance at the cathode by the simplified energy balance

$$j_c^+ V_c = j_c^- \phi + E_c \ .$$

Using the evaporation power they show that the evaporation (E_c) can account for most of the input energy ($j_c^+ V_c$) at a temperature that would give a negligible thermionic energy contribution ($j_c^- \phi$) for low melting point cathodes. Thus they conclude that thermionic emission does not seem to be important for low melting point cathodes.

3.1.3 Llewellyn Jones

The energy dissipation at both electrodes is analyzed by Llewellyn Jones[30]. He assumes this energy is composed of evaporation energy (including melting before evaporation), radiation and conduction (M + E + R + C = energy dissipated). After simplifications, this equation reduces to the volume of metal evaporated in terms of three unknowns, one being the effective capacity of the energy dissipated (M + E + R + C). Using data from erosion of spark plugs from three metals of known, preferably widely differing, physical properties--and assuming that this erosion is from evaporation--, the effective capacity of the energy dissipated was determined. This capacity was found to be about 11% of the total capacity of the gap. The other 89% of the energy in the gap, therefore, must go to gaseous processes and energy required to emit electrons.

Llewellyn Jones also gives an upper estimate of the time required to raise the hot-spot temperature to the boiling point. This is done

by considering the rise in temperature of the surface of an infinite metal plane due to a constant heat input. This estimate is to ensure that enough time is available in a normal arc discharge. Arcs usually range from times of 1 μ sec. to 1 m sec. The temperature rise θ^o after a time t is given by the equation

$$\theta^o = 2Q \left[\frac{t}{\pi k c \rho}\right]^{1/2} \qquad \text{with} \qquad \left[\frac{r^2 c\rho}{kt}\right]^{1/2} >> 1$$

where k = thermal conductivity

c = specific heat

ρ = density

Q = energy supplied per unit area

r = radius of spot

For nickel with $\theta \simeq 3000^o$, $kc\rho \simeq 1$, and an arc with current density of $\simeq 10^6$ a/cm^2, the ion current density may be taken as 10^5 a/cm^2 and the cathode fall ≃ 20 volts. This gives a $Q \simeq 2 \times 10^6$ watts/cm^2 at the cathode and $\simeq 2 \times 10^7$ watts/cm^2 at the anode. The values of t calculated are 3×10^{-5} sec. for the cathode and 3×10^{-7} sec. for the anode. These times therefore can be neglected as compared to the majority of the times of an arc.

3.1.4 Somerville, Blevin and Fletcher, and Blevin

Two other papers that seemingly contradict those of Cobine and Burger[24] and Llewellyn Jones[30] are papers by Somerville, Blevin and Fletcher[7], and Blevin[9]. Cobine and Burger determined that the temperature of the anode is above its boiling point, and Llewellyn Jones assumed the temperature of both the electrodes were at their boiling points.

But the latter two papers determined that the temperatures of the electrodes are considerably above the melting point, although they are much less than the boiling point of the electrodes. Somerville, Blevin and Fletcher, and Blevin all use the same approach in analyzing the erosion of electrodes. They assumed that linear heat flow existed with melting of the electrodes. By using layers of thin foil as the electrodes, they observed the depth of melting. Then by assuming this depth has obtained the melting point temperature and, using an appropriate heat transfer solution, they determined the surface temperature. Blevin calculated the anode temperature of tin to be about 1500 ^{o}C compared to Somerville, Blevin, and Fletcher's value of about 900 ^{o}C for the cathode temperature. An indication of the anode temperature being approximately 70% higher than the cathode temperature was that the crater on the anode was about twice as deep as the crater on the cathode.

From the temperature profile Blevin determined the heat flux to the anode. Blevin says that this energy flux would represent an anode fall of 2 to 9 volts. These values are in agreement with observed values, although Blevin does not give the details of his calculation.

Somerville[23] tries to reconcile the apparent contradiction of the previous four papers. He says that vaporization need not take place if an arc duration is very short, or if the anode is efficiently cooled, or if the current is small. These restrictions may apply because Cobine and Burger[24] do use much greater currents and somewhat longer arcs than does Blevin[9], 11,000 amps and 1/120 sec. compared to 50 amps and 1 μ sec. to 1 m sec.

3.2 Energy Balance at Electrodes Applied to EDM

The two distinct methods that are employed in EDM will be described below, in order to describe the energy balances directly in terms of the observations made of EDM. The first method used in EDM is one in which the tool is the cathode (called standard polarity EDM), and in the second method the tool is the anode (called reverse polarity EDM). Standard polarity is used for high frequency machining (frequency > 2 Kc or arc durations < 500 μ sec.) and results in greater anode erosion than cathode erosion. When reverse polarity is used with arc discharge durations greater than 500 μ sec., a higher energy pulse is produced than when using standard polarity at the same current. In reverse polarity, when using high energy pulses (long duration and/or high currents) and large gap distances, the erosion of the anode decreases, and in extreme conditions cathode material is deposited on the anode.

In order to examine the extreme conditions between standard and reverse polarity EDM, the following anode-cathode combinations will be analyzed:

	1	2	3	4
Cathode:	Cu	C	C	Cu
Anode:	Cu	C	Cu	C

Conditions 1 and 2 will be studied to determine the distribution of arc energy to each electrode using the same material for each electrode. The difference between conditions 1 and 2 is that carbon (C) is a refractory metal and therefore has a much lower current density than copper (Cu) (see Section 2.2.2). Condition 3 is similar to what is used for

standard polarity EDM, although steel is usually the anode instead of copper. Copper is used instead of steel or iron because it is easily accessible in pure (99.99%) form. Also, copper, as well as iron, gives the same characteristic of a high current density. The main difference between iron and copper is that copper has a much higher thermal conductivity; however, this will not hinder the comparison between copper and carbon when discussing the arc characteristics. In reverse polarity EDM, carbon (graphite) is usually employed as the anode (tool), as in condition 4 above.

The energy balances for condition 1, Cu cathode - Cu anode, will be done in detail, whereas the remaining calculations for conditions 2 to 4 will just be tabulated.

The energy balance at the cathode from above is

$$j_c^+(V_c + V_i + V^+ - \phi) + R_G = j_c^-\phi + M_c + E_c + R_c + C_c \ .$$

Combining R_G and R_c and solving for $M_c + E_c + C_c$, we get the energy available for conduction, melting, and evaporation.

$$M_c + E_c + C_c = j_c^+(V_c + V_i + V^+ - \phi) + (R_G - R_c) - j_c^-\phi \ .$$

Using the values given in Chapter 3 for copper,

$$M_c + E_c + C_c = 10^5 \text{ amp/cm}^2 \ (10 + 7.68 + 0.8 - 4.38) \text{ volts} + 7321 \text{ watts/cm}^2 -$$

$$= 1.41 \times 10^6 + 7.321 \times 10^3$$

$$\cong 1.417 \times 10^6 \text{ watts/cm}^2$$

where $(R_G - R_c) = \sigma[(6000\ ^oK)^4 - (1356\ ^oK)^4]$ watts/cm^2

$(\sigma = 5.67 \times 10^{-12}$ watts/cm^{2}deg^{4}K)

$= 7.321 \times 10^3$ watts/cm^2

and $V^+ = \frac{3}{2} kT = \frac{3}{2} \frac{1.38 \times 10^{-23}\ j/K)}{1.6 \times 10^{-19}\ j/ev} 6000\ ^oK \cong 0.8$ volts

which is just the kinetic energy of an atom at 6000 ^oK.

The omission of the $j_c^- \phi$ term should be noticed in the previous calculation. This term represents the electron cooling term caused by the electrons surmounting the work function barrier in thermionic emission. But since the probable mechanism for electron emission using low melting cathodes is field emission, and not thermionic emission, this term can be neglected. It can be neglected because electrons emitted by field emission do not have to surmount the work function barrier.

The values used in the above calculations as well as those which will be used in Tables 1 and 2 were the averaged values reported in Chapter 3. Examples of these average values are given as follows: Since the anode fall potential for low melting point metals was given to range from 2 to 9 volts in Section 2.2.1, the average anode fall potential is 5.5 volts. This value of 5.5 volts was rounded off to 5 volts for the previous calculation because lower than average anode fall potentials are expected for the small gap spacing encountered in EDM. Other average values used in the previous calculations were 10^6 a/cm^2 for the electron current density at the cathode and 10^5 a/cm^2

for the electron current density at the anode. These values for the current densities were reported in Section 2.2.2. It should be noticed that the anode current density used is the highest value of the range reported in Section 2.2.2. This high value was used because it is believed that the anode current densities experimentally determined will give low values. Low values for the anode current density are expected because of the problems encountered in measuring the area of the arc channel or in measuring the eroded crater made by the arc. These are the same problems discussed in Section 2.2.2 for measuring cathode current densities.

Care must be taken here to notice that the energy balance equations are actually equating energy per time per area or power per area, which by convention is called energy density. Since the total power equals the total voltage (V) times the current (I), we can determine what percentage of this energy goes into the cathode for conduction, melting, and evaporation.

Because the gap distances are very small, the voltage potential across the plasma column is negligible (see Section 2.2.4.1), which means that the total voltage approximately equals $V_c + V_a$; therefore,

$$\begin{aligned} \text{arc power} &= IV \\ &= (j_c^+ + j_c^-)\, A_c\, (V_c + V_a) \\ &= (j_c^+ + 10\, j_c^+)\, A_c\, (V_c + V_a) \\ &= 11\, j_c^+\, (V_c + V_a)\, A_c \end{aligned}$$

Thus the percent of the arc energy that goes into the cathode for conduction, melting, and evaporation is

$$\%_c = \frac{(M_c + E_c + C_c)A_c}{11\, j_c^+(V_c + V_a)A_c} = \frac{(M_c + E_c + C_c)}{11\, j_c^+(V_c + V_a)} \quad .$$

For copper this gives

$$\%_c = \frac{1.413 \times 10^6}{11(1 \times 10^5)(10 + 5)} \cong 9\% \quad .$$

The energy balance at the anode for the Cu cathode - Cu anode combination is as follows:

$$j_a^-(V_a + \phi + V^-) + R_G = M_a + E_a + R_a + C_a \quad .$$

Rearranging

$$\begin{aligned} M_a + E_a + C_c &= j_a^-(V_a + \phi + V^-) + (R_G - R_a) \\ &= 10^5(5 + 4.38 + 0.8) + 7321 \\ &= 1.018 \times 10^6 + 7.321 \times 10^3 \\ &\cong 1.025 \times 10^6 \text{ watts/cm}^2 \quad . \end{aligned}$$

Putting the total arc power in the form $IV = j_a^- A_a(V_c + V_a)$, the percentage of arc energy going into the anode is

$$\%_a = \frac{(M_a + E_a + C_a)A_a}{j_a^-(V_c + V_a)A_a} = \frac{(M_a + E_a + C_a)}{j_a^-(V_c + V_a)}$$

$$= \frac{1.025 \times 10^6}{10^5(10 + 5)} \cong 68\% \quad .$$

The following two tables (number 1 and 2) give the results of the calculations for the four conditions.

3.2.1 Cu Cathode - Cu Anode Analysis

Using Cu for the cathode and anode gives rise to a very large energy density at both the anode and cathode. From Table 2 we can see that the area covered by the anode spot is about eleven times that covered by the cathode spot. The areas depicting the electrode spots in Table 2 were determined by the relative current densities to each electrode. For Cu electrodes the current density is 1.1×10^6 a/cm^2 to the cathode and 10^5 a/cm^2 to the anode. Since the same current exists at the cathode and anode, the area ratio of the cathode spot to the anode spot would be 1 to 11. This means that although the energy density to the anode is a little less than that received by the cathode, the energy given up to the anode represents 68% of the arc energy. By noticing that the energy to the electrodes by radiation is only a very small fraction (less than 1%) of the total energy, the assumption of black-body radiation will not produce any significant error in the calculation of the energy density for a low melting cathode.

Another important result that we can obtain from knowing the energy densities is the time needed to raise the surface temperature up to its melting or boiling point. This can be done by using the equation for one-dimensional heat transfer to a surface which was used by Llewellyn Jones in Section 3.1.3. This equation for the time needed to heat up a surface from T_o to T is

$$t = \frac{\pi k c \rho}{4} \left(\frac{T - T_o}{Q}\right)^2 .$$

For Cu: $\frac{\pi}{4} kc\rho = \frac{\pi}{4} (0.94 \frac{cal}{cm\,^oC\ sec})(0.092 \frac{cal}{gm\,^oC})\ 8.96 \frac{gm}{cm^3} (\frac{4.18\ watt\ sec}{cal})^2$

$$= 10.6 \left(\frac{watt}{cm^2\,^oC}\right)^2 sec$$

$$T_M - T_o = 1356\ ^oK - 298\ ^oK = 1058\ C^o$$

T_M = Melting temp.

The time to heat up the anode to its melting point is

$$t_{M_a} = 10.6 \left(\frac{1058}{1.025 \times 10^6}\right)^2$$

$$\cong 11\ \mu\ sec\ .$$

3.2.1.1 Cu Cathode - Cu Anode Experiments

Experiments performed on the Elox EDM machine by Viswanathan[6] show that the anode erodes more than the cathode. A series of tests covering frequencies from 1kc to 32 kc gave the following results. With the tool as the anode, the ratio of anode to cathode erosion increased from greater than 1 at 1 kc to greater than 6 at 32 kc. These tests were run at an average current of 35 amps and for a duty cycle (percent on time of discharge) of 50%. The lower percentage of anode to cathode erosion at 1 kc compared to that existing at 32 kc will be explained in Chapter 4 as arising from cathode metal being plated on the anode.

Condition	Current[a] Density (a/cm^2)	Electrode[a] Fall Potentials (V)	Radiation[b] to Electrode ($watts/cm^2$)	$j_c^-\phi$ $watts/cm^2$	Cathode Energy Balance[c] $M_c+E_c+C_c = j_c^+(V_c+V_i+V^+-\phi)+(R_G-R_c)-j_c^-\phi$	Anode Energy Balance $M_a+E_a+C_a = j_a^-(V_a+\phi+V^-)+(R_g-R_a)$
[1]Cu Cathode	$j_c^- = 10^6$ $j_c^+ = 10^5$	$V_c = 10$	7.321×10^3 (1356 °K)	0	$10^5(10+7.68+0.8-4.38)$ $+7.321 \times 10^3-0$ $= 1.417 \times 10^6$	$10^5(5+4.38-0.8)+7.321$ $\times 10^3 = 1.025 \times 10^6$
Cu Anode	$j_a^- = 10^5$	$V_a = 5$	7.321×10^3 (1356 °K)	0		
[2]C Cathode	$j_c^- = 10^3$ $j_c^+ = 10^2$	$V_c = 10$	3.52×10^3 (5100 °K)	4000	$10^2(10+11.2+0.8-4)$ $+(3.52-4.0)\times10^3$ $= 1.3 \times 10^3$	$10^2(12+4+0.8)$ $+6.2 \times 10^3$ $= 7.9 \times 10^3$
C Anode	$j_a^- = 10^2$	$V_a = 12$	6.2×10^3 (3808 °K)	0		
[3]C Cathode	$j_c^- = 10^3$ $j_c^+ = 10^2$	$V_c = 10$	3.52×10^3 (5100 °K)	4000	$10^2(10+11.2+0.8-4)$ $+(3.5-4.0)\times10^3$ $= 1.3 \times 10^3$	$10^2(12+4.38+0.8)$ $+7.321 \times 10^3$ $= 9.0 \times 10^3$
Cu Anode	$j_a^- = 10^2$	$V_a = 12$	7.321×10^3 (1356 °K)	0		
[4]C Anode	$j_a^- = 10^5$ $j_c^- = 10^6$	$V_a = 5$	6.2×10^3 (3808 °K)	0	$10^5(10+7.68+0.8-4.38)$ $+ 7.321 \times 10^3-0$ $= 1.417 \times 10^6$	$10^5(5+4+0.8)$ $+ 6.2 \times 10^3$ $= 9.86 \times 10^5$
Cu Cathode	$j_c^+ = 10^5$	$V_c = 10$	7.321×10^3 (1356 °K)	0		

a, b, c (see next page)

Table 1 - Energy Balance Calculations

[a]Average values given in Chapter 3.

[b]Radiation from assumed 6000 ^{o}K gas and melting and boiling temperatures of:

Cu	1356 ^{o}K;	2868 ^{o}K
C	3808 ^{o}K;	5100 ^{o}K

[c]V_iCu = 7.68 ϕ_{Cu} = 4.38

V_iC = 11.2 ϕ_{C} = 4.00

CONDITION 1		AREA		CONDITION 4	
Cu - 1.417×10^6 watt/cm^2	9%	$\frac{A_1}{11,000}$	Cathode	Cu - 1.417×10^6 watt/cm^2	9%
Cu + 1.025×10^6 watt/cm^2	68%		Anode	C + 9.86×10^5 watt/cm^2	66%
		$\frac{A_1}{1000}$			
CONDITION 2		$\frac{A_1}{11}$	Cathode	CONDITION 3	
C - 1.3×10^3 watt/cm^2	5%			C - 1.3×10^3 watt/cm^2	5%
C + 1.68×10^3 watt/cm^2	76% (excluding radiation)			Cu + 1.7×10^3 watt/cm^2	77% (excluding radiation)
7.9×10^3 watt/cm^2	360% (see text for discussion)			9.0×10^3 watt/cm^2	350% (see text for discussion)

Area = A_1

For same total current see area ratios above.

Anode

Table 2 - Relationships Between Energy Densities, percent Energies to Electrodes and Area Ratios

In experiments done by Doret[3], on the single-discharge apparatus, greater anode erosion than cathode erosion was also observed. In tests run at 50 amps and for arc durations of 13 to 3200 μ sec., the anode to cathode erosion ratio ranged from 1 to 4. Unfortunately this series of tests were run at a gap spacing of 0.005" which means that cathode metal will be plated on the anode. This plating, which produces a lower anode to cathode erosion ratio than expected, will be discussed in Chapter 4.

From the analysis in the previous section, it was determined that the energy impinging on the anode was about eight times greater than the energy impinging on the cathode. Thus it might be expected that the anode should erode eight times as much as the cathode. This expected result is in very good agreement with the above experiments if the problems discussed below are considered.

If it is assumed that the anode craters are formed by melting, the energy required for this melting amounts to only 5% of the arc energy. This percentage is far below the 68% predicted in the previous section. A number of possible reasons explaining the disagreement of these figures will be stated below. There is much more experimental work to be done on the amount of erosion produced under various conditions. Because of this lack of data, only a qualitative analysis comparing the above two figures will be done at this time.

One cause that accounts for some of the loss of energy is the conduction of heat occurring when the surface is being raised up to its melting point. This loss is increased if the arc spot moves over the anode surface.

An error that may account for a large part of the differences in the above figures is that a significant amount of the metal removed may have been evaporated. Also, if some of the molten metal was not ejected from the crater, its resolidification would cause an apparent reduction in erosion.

A series of tests[3] on the single-discharge apparatus was run to show the increased erosion of the anode from a 13 μ sec. to a 3200 μ sec. discharge. The extremely small crater produced with the 13 μ sec. discharge agreed with the estimation of the time needed to raise the surface to its melting point. This was calculated to be 11 μ sec. in Section 3.2.1. The tests from 13 μ sec. to 3200 μ sec. show a definite increase in erosion with time.

A good illustration of the erosion caused by the arc is seen in Fig. 4b. This photograph of the eroded surface shows that the arc has travelled across the surface. The arc seems to have stopped moving three times in travelling across the surface, thus forming three craters. It should be emphasized that the voltage and current traces for this discharge were very clear and constant, thus assuring us that these three craters were made by a continuous arc. An additional assurance of the existence of a single arc is given by the slight path eroded between the top two craters.

3.2.1.2 Fe - Cu Cathode-Anode Combinations

Since Fe and Cu are both low melting point metals, they both produce high-energy densities when used as cathodes. Also, the time needed to heat Fe to its melting point is similar to the time required for Cu,

i.e., 5 μ sec. compared to 11 μ sec., and since the latent heat of fusion for Fe (65 cal/gm) is not too much greater than for copper (50.6 cal/gm), it should be expected that the erosion for Fe should be similar to that of Cu.

In standard polarity EDM, at short arc durations, the Fe anode erodes three to four times as much as the Cu cathode[6]. This is in agreement with the observations made using a Cu cathode and anode stated in the previous section. An unexpected result occurs when the energy liberated per discharge is increased. This increase in energy, which can be accomplished in many ways, increases the gap spacing between the electrodes. The unexpected result is the reduction of Fe anode erosion. The cause of reduction can be seen when the energy discharged per pulse, or the gap spacing, is increased still further. At this time, plating from the Cu cathode onto the Fe anode is observed. This plating which causes an apparent reduction of anode erosion will be discussed in Chapter 4.

Since this protection of the anode takes place, it is used to an advantage by switching polarities and using the tool as the anode. This is called reverse polarity EDM and results in more Fe cathode erosion than Cu anode erosion. In fact, at very large gap distances[4], instead of having anode erosion, a build-up of Fe on the anode is observed. These large gap spacings may be as high as 0.005"to 0.007". Unfortunately the exact gap spacings can only be estimated as being less than the overcut which is 0.005" to 0.007". The overcut is the clearance between the tool and workpiece that has been eroded during

machining. The overcut is an upper limit for the gap spacing, since eroded particles between the tool and workpiece may be in contact with either the tool or the workpiece. Thus the arc discharge could be formed between the eroded particle and the other electrode.

3.2.2 C Cathode - C Anode Analysis

The most important difference between carbon and copper electrodes is that the carbon cathode has a much lower current density (see Section 2.2.2). This low-current density accounts for the extremely low-energy densities impinging upon the carbon electrodes.

An error results if the radiation is included in the analysis for the percent of arc energy to the anode. The error is that three and one-half times more energy would be received by the anode than supplied by the arc. This result means that the assumption of blackbody radiation is not valid for this analysis. But even with this error, the enormous difference between the energy densities of low melting point cathodes (Cu) and refractory cathodes (C) is not altered.

Neglecting radiation, the time needed to raise the anode surface up to the melting temperature was calculated to be 1.25 sec. This means that with a carbon cathode no erosion should occur on the anode for arc durations less than 1.25 sec.

3.2.2.1 C Cathode - C Anode Experiments

In the few experiments[3,5] done with C cathode - C anode combinations, negligible erosion occurred. The electrode surfaces seem either to be scorched or roughened by mechanical erosion. Since carbon (graphite) is very soft, the slight erosion observed might be from mechanical erosion.

3.2.3 C Cathode - Cu Anode Analysis

Since the characteristics of the arc are determined by the cathode, this analysis is similar to the analysis above. The time required to heat the anode surface to its melting point temperature was determined to be 4.1 sec; therefore, in the arc durations encountered in EDM, there should not be any erosion of a copper anode with a carbon cathode. But we know that there is a great deal of erosion under these conditions in EDM. In fact, this is the condition for standard polarity EDM, although steel would be the anode instead of copper.

Thus we are faced with the problem of explaining observed erosion which the arc analysis cannot explain. This problem has been solved in the following way. If a refractory cathode is used, the erosion produced on the anode is caused by the initiation of the arc (i.e. spark). This means that the erosion in EDM using a carbon cathode (standard polarity) is caused by spark erosion. The strength of the spark is supported by work done by Sigmond (see Appendix B). Sigmond states that the current at the refractory (tungsten) cathode during a nanosecond arc is greater than 10^6 a/cm^2. Along with this high current density impinging on the anode, Somerville[54] states that a shock wave is present during the spark phase of an arc.

It is concluded that the spark's high current density and shock cause erosion on the anode. This conclusion is supported in the following section by observing that the erosion during a 13 μ sec. arc is only slightly less than the erosion during a 3.2 m sec. arc.

3.2.3.1 C Cathode - Cu Anode Experiments

It was observed[3] that arc discharges ranging from durations of 13 μ sec. to 3.2 m sec. showed only very slight increases in anode erosion. To further show that negligible erosion occurred after 13 μ sec., or after the spark, some tests were performed for arc durations of a few seconds. These tests also showed one small crater similar to the crater formed under 13 μ sec. After a few seconds slight melting also occurred over a large area of the anode surface. This slight melting supports the analysis of arc erosion occurring after approximately four seconds. Another point can be made about these long arc discharges. This point is that with a carbon cathode only one distinct crater is observed on the anode (Fig. 4c, d). This can be compared to the many distinct craters observed using a copper cathode (Fig. 4b). The appearance of only one crater, using the carbon cathode, also illustrates that it was formed at the initiation of the arc. Even for the tests that were run for several seconds, and moving the arc around the surface while the arc was on, only one crater was observed.

3.2.4 Cu Cathode - C Anode Analysis

With copper as the cathode, this analysis should be similar to the Cu cathode - Cu anode analysis. This means that the energy densities at the electrodes are enormously high compared to the condition when a carbon cathode was used. The analysis predicts that 66% of the arc energy will impinge upon the anode with an energy density of 9.86×10^5 watts/cm^2. The energy received by the cathode was calculated

to be about 9% of the arc energy, representing an energy density of 1.417×10^6 watts/cm^2. With these energy densities the times needed for the Cu cathode and the C anode to reach their melting points are 6 μ sec. and 4 μ sec., respectively.

Although the carbon cathode would seem to melt from the above calculation, it does not for the following reason: Graphite does not liquify at pressures under 100 atmospheres. And since the latent heat of vaporization is so great, significant sublimation is not possible.

Because the Cu cathode receives the same energy as received in condition 1 (i.e., Cu cathode and anode), the same erosion is expected in both conditions.

3.2.4.1 Cu Cathode - C Anode Experiments

A small amount of erosion was observed on the C anode. The erosion seems to be mechanical erosion. Although this C erosion is not significant for one discharge, it could be significant in the machining process with repeated discharges.

Unfortunately, only a limited number of machining tests[6] have been made with a Cu cathode and a C anode. But the following results will be stated for a Fe cathode and a C anode. From the limited number of tests that have been run, Cu gives similar results to Fe.

When machining steel (Fe), the C anode erosion is fairly constant until large gap spacings are used. At those spacings plating of the Fe cathode onto the C anode is seen[4]. This is the same result that was discussed in Section 3.2.1.2 for Fe plating onto the Cu anode.

3.3 Conclusions From Energy Balance at the Electrodes

The immense value of studying EDM, using the energy balance at the electrodes, is shown by the numerous conclusions stated below.

By using the energy balance, it was determined that much more energy is imparted to the anode surface than the cathode surface. The percentage of the total arc energy delivered to the anode and cathode was calculated to be approximately 70% and 7%, respectively. However, if the electrode erosion is assumed to be caused by melting, only 5% of the total arc energy would be required. This experimentally determined value of 5% could be reconciled to the calculated value of 77% if vaporization and/or resolidification of molten metal is present.

Because of the low-energy density produced by a carbon cathode, it was determined that a carbon arc could not cause significant electrode erosion for the arc durations encountered in EDM. Thus it is concluded that most of the erosion was caused by the initiation of the arc, or the spark.

This spark erosion, with a carbon cathode, is contrasted to the long duration arc erosion produced by a low melting point cathode.

One observation that the energy balance at the electrodes cannot explain is the following: This is the apparent reduction of anode erosion caused by the plating of a low melting point metal on the anode. An explanation of this plating will be given in the following chapter.

All of the above conclusions have been verified experimentally, although the number of experiments performed has been limited.

4.0 GAS AND EROSION JETS

In the preceding chapter the analysis of anode erosion using a low melting point cathode did not agree with the experimental results. The disagreement occurs with high-energy discharges and large gap distances. The analysis predicts that the anode erosion should increase with increasing energy. But a reduction in erosion is observed in EDM, and in extreme conditions a build up of cathode material on the anode results.

In Section 4.1 a mechanism will be proposed that can explain this apparent reduced erosion by the plating of cathode material on the anode. It is believed that this plating results from the cathode metal, in its vapor and molten state, being propelled by gas jets to the anode. These gas jets are described by Maecker[55] as arising from the arc's self-magnetic field.

Our theory does not explain how the molten cathode metal is initially ejected. Although there is no established theory of how the molten metal is ejected from the cathode surface, we present two possible theories.

The question of how the molten cathode metal is initially ejected is a very important problem to be solved. At present, a more important question is to know when the molten cathode metal is ejected. Unfortunately this problem has not been resolved. If the molten metal is ejected during the arc, we shall show that Maecker's gas jets can propel this molten metal to the anode. But if most of the metal is ejected after the discharge has ended,

Maecker's gas jets could not propel this metal. However, even if only a small fraction of the eroded cathode metal is ejected during the arc, it may still be the predominant metal that is plated on the anode.

Also presented in this chapter are erosion jets that occur in several different types of discharges. These jets of eroded electrode metal are discussed with the hope that they may increase our understanding of any erosion jet that may occur in EDM.

4.1 Plating of Cathode Metal on Anode by Maecker's Gas Jets

Because of the build up of cathode metal on the anode, we propose that this is accomplished by Maecker's gas jets. Before the details of our theory are given, we shall present Maecker's theory and experimental evidence to support same in Sections 4.1.1 through 4.1.3.

4.1.1 Maecker's Gas Jet Theory

Maecker's theory[55] of gas jets emanating from the electrodes does not mean that there is erosion from the electrodes. But if there is erosion, Maecker's gas jets will propel the eroded particles or vapor away from the electrodes. Somerville[56] says that Maecker has shown that the gas jets from the electrodes arise from the compressive forces exerted on the arc by its own magnetic field. Since this magnetic compressive force increases as the current density increases, it will be greatest in the constriction at the electrodes; therefore, a pressure gradient will be set up normal to and directed away from the electrode. This gas jet can even exist without

vaporization since the surrounding gas is sucked into the jet and propelled away from the electrodes. As a consequence of the compressive force increasing with current density, the gas jet emanating from the cathode is much greater than the jet coming from the anode, since the cathode current density is usually one or two orders of magnitude greater than the anode current density.

Maecker derived the following expression for the maximum pressure occurring on the axis of the arc that balances the magnetic forces which are produced by the arc.

$$p_{max} = \frac{\mu_o}{4\pi} IJ = \frac{\mu_o}{4\pi} \frac{I^2}{(Area)}$$

Thus the maximum gage pressure is directly proportional to the total current and current density. (See Appendix A for Maecker's detailed analysis.) By solving the equation of motion for the arc, Maecker determined that the maximum velocity that the gas jet could attain was equal to

$$v_{max} = \sqrt{\frac{2\, p_{max}}{\rho}} \quad .$$

4.1.2 Maecker's Gas Jet Experiments

From the above expression for the maximum pressure, we realize that the pressure is inversely proportional to the cross-sectional area of the arc. To show the existence of a gas jet from a constriction in the arc, Maecker placed a nozzle in the center of the arc. Because of the constriction caused by the nozzle, a plasma

disk was formed between the nozzle and the cathode. This disk resulted from the collision of the gas jet formed by the nozzle and the gas jet emanating from the cathode constriction. With the gas jets sucking gas in from their origin, i.e., at the constriction, a vacuum exists at the constriction. Maecker measures the presence of this vacuum by attaching a manometer to a double nozzle.

Another experiment performed by Maecker which is directly applicable to what we shall propose in Section 4.1.4 is the following: Maecker placed small carbon particles in the vicinity of the cathode. Upon doing this, the particles were sucked into the cathode jet and propelled toward the anode. After hitting the anode the particles were reflected to the side by the incoming gas jet.

The recoil force, caused by the momentum of the gas jet, was also calculated by Maecker. (See Appendix A for the details of this calculation.) The magnitude ($\sim$ 1 gm weight) and current dependence ($F_c = \frac{\mu_o}{4\pi} I^2 \ln \frac{r_s}{r_c}$) of the recoil force agreed with work done on gas jets by other investigators.

Maecker did most of his experiments with a carbon cathode because of its stability. But he does show some photographs of a gas jet coming from a low melting point cathode (copper). He says that the copper cathode arc is less stable than the carbon cathode arc because of a gas jet emanating from the anode. With the information given in Section 2.2.2, we would expect this result to occur. Section 2.2.2 states that with the much higher cathode current density for copper than

carbon, a larger current density at the copper anode will result. With this high current density at the anode, we would expect a gas jet to be present. We also expect a much stronger gas jet at the copper cathode than at a carbon cathode, which would contribute to the instability observed by Maecker for a copper cathode.

4.1.3 Mandel'shtam and Raiskii Gas Jet Experiments

In an effort to explain the mechanism of electrical discharge machining, Mandel'shtam and Raiskii[57] propose that the electrode erosion is caused by mechanical action of metal-vapor jets. Since these vapor jets occur during the arc discharge, they are of the type described by Maecker. Although the Mandel'shtam and Raiskii erosion theory is not generally accepted, they do present some of the characteristics of vapor jets (or gas jets). Using photographs they show that the gas jet from the cathode is greater than the gas jet from the anode. Mandel'shtam and Raiskii also describe the process used in electrical discharge machining with reverse polarity (workpiece negative). They say that with greater gap distances than are used with standard polarity, greater erosion occurs on the cathode than the anode. It is also observed that a build up of cathode material sometimes occurs on the anode for these larger gap distances. The observations were made for arcs in air and in a liquid dielectric. The only apparent difference in using a liquid was an increased erosion in the liquid.

4.1.4 Proposed Theory to Explain the Effect of Maecker's Gas Jets on the Plating of the Anode

In the following proposed theory, Maecker's gas jet will be shown to be a sufficient force for the propelling of cathode vapor and liquid

to the anode. At the present time, it is not known with any certainty how the molten cathode metal is initially ejected from the cathode surface. Also, a good explanation has not been given describing how the plating is accomplished when the molten cathode metal impinges on the anode. Barash and Kahlon[38] give us an indication that vapor or liquid of a certain melting point metal can be plated on a lower melting point metal. In fact, they state (see Section 2.2.4.1) that plating onto the lower melting point metal gives more plating than vice versa. This condition is observed in their study of electrical discharge hardening.

4.1.4.1 Influence of Gas Jets at Large Gap Spacings

From experiments done on an EDM machine, it seems that increased plating of cathode metal on the anode occurs at large gap spacings, i.e., 0.005 to 0.007 in. This dependence was shown in a thesis done by Juvkam-Wold[4] at M.I.T. Unfortunately, it still has to be mentioned that this increased plating was also a function of the energy delivered per discharge. The latter dependence is present because the increased gap spacings are dependent on increased energy delivered per discharge in the EDM machine used.

The influence of the gas jets on gap spacing will be described by examining the arc profile. Fig. 5 shows the profile at gap spacings of 0.005 in and 0.001 in. These profiles of a 50 amp arc assume current densities of $j_c = 1.1 \times 10^6$ a/cm^2 and $j_a = 10^5$ a/cm^2.

The following diagrams will be used as approximations of those profiles.

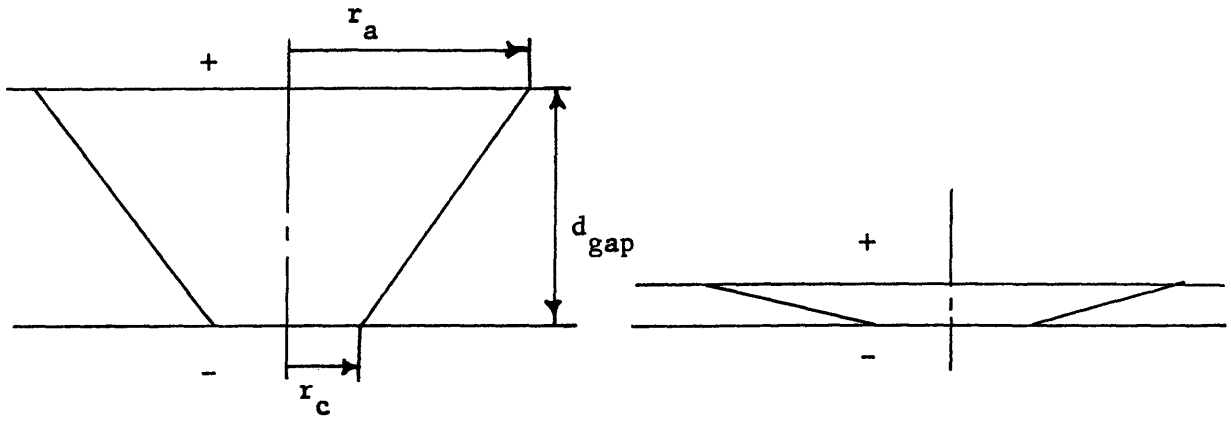

Gap Spacing = 0.005" Gap Spacing = 0.001"

In examining Fig. 5 and the above diagrams, it is suggested that a gap spacing of 0.001" is not sufficient for the formation of a gas jet from the cathode to the anode. It seems that the small gap spacing would not allow gas to be sucked into the arc at the cathode spot. But with the larger gap spacings (0.005" to 0.007"), the expansion from the cathode spot to the anode spot does not seem too severe.

As a measure of the degree of expansion from the cathode spot to the anode spot, an expression for the slope of line joining the two radii will be developed.

$$\text{Slope} = m = \frac{d_{gap}}{r_a - r_c}$$

$$= \frac{d_{gap}}{\sqrt{\frac{A_a}{\pi}} - \sqrt{\frac{A_c}{\pi}}}$$

$$= \frac{d_{gap}}{\sqrt{\frac{A_c}{\pi}}\left(\sqrt{11} - 1\right)}$$

$$m = 2.04 \times 10^3 \frac{d_{gap}}{\sqrt{I}}$$

Using

$$A_a = \pi r_a^2$$

$$A_a = 11\, A_c$$

For $j_c = 1.1 \times 10^6$ a/cm^2

$$j_a = 10^5 \text{ a/cm}^2$$

$$j_c = \frac{I}{A_c}$$

Plating on the anode is observed for currents and gap spacings greater than 50 amp and 0.005 in., respectively[5]. For this reason, the slope at 50 amp and 0.005 in. will be chosen as the lower limit for the influence of gas jets on the plating of the anode. Thus

$$m_{\substack{50\ \text{amp} \\ 0.005\ \text{in.}}} = \frac{2.04 \times 10^3\ (0.005\ \text{in.})}{\sqrt{50\ \text{amp}}} = 1.443$$

gives the value of the minimum expansion of the arc column for the gas jets to be effective.

But this expression, $m = 2.04 \times 10^3 \frac{d_{gap}}{\sqrt{I}}$, indicates that if the current decreases, a greater slope may be attained; therefore, using the minimum slope of 1.443, the gas jets should plate the anode at 0.001 in. if a current of 2 amp is used. This apparent contradiction to the previous statement, that gas jets are not effective at 0.001 in., can be explained by the following cause. Since the velocity of the gas jet is directly proportional to the square root of the current,

$$\text{i.e.,}\quad v_{max} = \sqrt{\frac{2\ p_{max}}{\rho}} = \sqrt{\frac{2\ \mu\ j}{\rho\ 4\ \pi}\ \ I}\ ,$$

$$\text{with}\quad p_{max} = \frac{\mu_o\ I\ j}{4\pi}$$

the influence of the gas jet will be small at this low current.

Because a low current of 2 amps is seldom, if ever, used in industrial practice, the existence of gas jets at this low current is of little importance in EDM machining. Low currents are not used because the machining rate would be too low to be economical.

The slope of the line connecting the cathode and anode spots (m) decreases with increasing current. With this dependence, the gas jet at 50 amp and 0.005 in. gap would seem to be hindered if the current were increased. This effect is not present in EDM machines because as the current is increased, the gap spacing increases. The increased current causes a greater energy per discharge to be liberated. This greater energy results in larger particles to be eroded, which in turn, makes the arc breakdown at larger gap spacings.

Another effect which reduces the significance of the decreasing slope, that is not dependent on the EDM machine, is the following: The velocity of the gas jet increases with increasing current, therefore, increasing the gas jet's strength for plating.

4.1.4.2 Agreement Between Increasing Strength of Gas Jets and Observed Increased Anode Plating

There are many conditions that substantiate the increased strength of gas jets occurring when increased plating of the anode is observed. Unfortunately we do not have conclusive experimental evidence to state that the gas jets are the direct cause of the plating. The only conclusions that can be made with any certainty are that Maecker's gas jets can propel liquid metal particles and that the gas jet's increase in strength occurs at increased plating.

An important agreement between the strength of the gas jets and the plating of the anode is that the plating is from the cathode to the anode. Since the current density is greatest at the cathode, Maecker's theory shows that the gas jet from the cathode is much greater than the gas jet from the anode.

This agreement can be contrasted to the possibility of molten cathode metal being ejected after the discharge has ended. There seems to be a contradiction if we assume that cathode metal is plated on the anode after the discharge has ended. This contradiction arises from the analysis of the energy balance at the electrode, showing that more energy is received by the anode. If the anode and cathode have similar thermal properties, more metal should be ejected from the anode than the cathode. Thus it would be expected that more anode metal should be plated on the cathode than vice versa. But this is not the case. An example of what occurs in EDM is the plating of a steel cathode on a copper anode at large gap distances.

Another example showing the agreement between gas jets and anode plating is the fact that plating occurs when a low melting point cathode is used. The agreement concerns the fact that a high current density is caused by using a low melting point cathode. Because of the high current density, the gas jets are much stronger than if a refractory cathode, with its low current density, were used.

It should be noted that a strong agreement between Maecker's gas jets and anode plating was offered in the previous section. This was the condition that the gas jets could be more developed at larger gap spacings.

4.1.4.3 Propulsion and Heating of Cathode Liquid Metal by Maecker's Gas Jets

The maximum pressure and velocity of the gas jet will be determined for a 6000 ^{o}K arc column. The velocity of the gas jet will then be used to calculate the drag force on a 0.001" (2.54×10^{-3} cm)

diameter liquid metal sphere. This drag force will determine if the gas jet is able to accelerate the metal sphere across the gap spacing in the duration of a discharge.

Also the heating effect of the gas stream on the metal sphere will be analyzed. It will be determined if the duration of the arc is sufficiently long to heat the cathode metal sphere from its melting point to its boiling point.

The calculations will be made with the following conditions:

Copper Cathode

$T_{gas} = 6000\ ^{o}K$

$j_c = 1.1 \times 10^{6}\ a/cm^2$

$I = 50\ amp$

$d_{gap} = 0.005"$

The maximum pressure using Maecker's formulation is

$$p_{max} = \frac{\mu_o I j}{4\pi} = 4\pi \times 10^{-7} \frac{nt}{amp^2} \frac{(50\ amp)(1.1 \times 10^{10} \frac{amp}{m^2})}{4\pi} \frac{(14.7\ psi)}{10^5 \frac{nt}{m^2}}$$

$$= 8.08\ psi.$$

The maximum velocity is obtained by using this pressure.

$$v_{max} = \sqrt{\frac{2\ p_{max}}{\rho}} = \sqrt{\frac{2(5.5 \times 10^4 \frac{nt}{m^2})}{5.89 \times 10^{-5} \frac{gm}{cm^2}} \frac{10^3 gm}{Kg} \frac{m}{10^2 cm}}$$

$$= 1.37 \times 10^5\ cm/sec.$$

$$\text{where} \quad \rho = \frac{p}{RT} = \frac{14.7 \frac{\#}{in^2} \quad 144 \frac{in^2}{ft^2}}{53.3 \frac{ft\#}{\# \, {}^{o}R} \quad 10{,}800 \, {}^{o}R}$$

$$= 3.68 \times 10^{-3} \ \#/ft^3$$

$$= 5.89 \times 10^{-5} \ gm/cm^2 \ .$$

Before the drag is calculated, the flow regime must be determined.

For the hard sphere approximation, the Knudsen number (Kn) equals

$$K_n = \frac{\lambda}{D} \quad \text{where:} \quad \lambda = \text{mean free path}$$

$$= \frac{1}{\sqrt{2} \ \pi d^2 n}$$

$$d = \text{diameter of atom}$$

$$n = \text{number density} = \frac{\rho}{\text{mass}}$$

$$n = \frac{5.89 \times 10^{-5} \frac{gm}{cm^3} \quad 6.023 \times 10^{23} \ part}{14 \ gm} = 2.53 \times 10^{18} \ cm^{-3}$$

$$\lambda = \frac{1}{\sqrt{2} \ \pi \ (1 \times 10^{-8} cm)^2 (2.53 \times 10^{18} cm^{-3})} = 0.89 \times 10^{-3} \ cm$$

$$\therefore \ Kn = \frac{(0.89 \times 10^{-3} cm)}{(2.54 \times 10^{-3} cm)} = 0.35$$

Since the Knudsen number is close to one, the flow is in the beginning the free molecule flow regime; therefore, the drag (D) on the sphere is equal to $\pi r^2 \rho V^2$, which is the total momentum transfer on the projected area.

$$D = \frac{\pi d^2}{4} \rho V^2 = \pi \frac{(2.54 \times 10^{-3} \text{cm})}{4} \; 5.89 \times 10^{-5} \frac{\text{gm}}{\text{cm}^3} \frac{(1.37 \times 10^5 \frac{\text{cm}}{\text{sec}})^2}{980 \text{ cm/sec}^2}$$

$$= 5.71 \times 10^{-3} \text{ gm} .$$

Knowing this drag force, the acceleration of this 2.54×10^{-3} cm diameter copper sphere can be calculated.

$$a = \frac{D}{m} = \frac{5.71 \times 10^{-3} \text{ gm } 980 \frac{\text{cm}}{\text{sec}^2}}{7.68 \times 10^{-8} \text{ gm}} = 7.28 \times 10^7 \text{ cm/sec}^2$$

where m = mass of sphere

$$= \frac{\pi}{6} D^3 \rho = \frac{\pi}{6} (2.54 \times 10^{-3} \text{ cm})^3 \; 8.96 \frac{\text{gm}}{\text{cm}^3}$$

$$= 7.68 \times 10^{-8} \text{ gm} \quad .$$

The time necessary for this sphere to traverse a 0.005" gap with this acceleration is calculated as follows:

$$t = \sqrt{\frac{2d}{a}} = \sqrt{\frac{(2)(0.005")2.54 \text{ cm/"}}{7.28 \times 10^7 \text{ cm/sec}}} = 1.87 \times 10^{-5} \text{ sec.}$$

Thus the above shows that Maecker's gas jets can propel spheres up to 0.001" in diameter from the cathode to the anode. The previous calculation also determines that these spheres can be propelled well within the times encountered in arc discharges.

The heating effect of the 6000 ^{o}K gas jet on the sphere will now be analyzed. In order to calculate the heat transfer coefficient (h), the Mach number (M) will be calculated as follows:

$$M = \frac{v}{v_s}$$

where $v_s = \sqrt{\gamma RT} = \sqrt{(1.4)\ \ 53.3\ \frac{ft\#}{\#\ ^oR}\ 32.2\ \frac{ft}{sec^2}\ 10{,}800\ ^oR}$

$= 5.1 \times 10^3$ ft/sec

$= 1.55 \times 10^5$ cm/sec

$\therefore\ M = \frac{1.37 \times 10^5}{1.55 \times 10^5} = 0.88$.

Using Fig. 11.26 in Rohsenow and Choi[58], the Stanton number (St) can be determined if the speed ratio ($s = \sqrt{\frac{\gamma}{2}}\ M$) is known.

With $s = \sqrt{\frac{\gamma}{2}}\ M_\infty = \sqrt{\frac{1.4}{2}}\ (0.88) = 0.737$

$$\frac{1}{A}\ \frac{\gamma}{\gamma + 1}\ St = 0.22$$

A = thermal accommodation coefficient = 0.92

therefore,

$$h = St\rho Vc_p = 0.22\ \frac{\gamma + 1}{\gamma}\ A\ \rho Vc_p$$

$= (3600\ \frac{sec}{hr})\ 0.22\ \frac{2.4}{1.4}\ (0.92)\ 3.68 \times 10^{-3}\ \#/ft^3\ 1.37 \times 10^5\ \frac{cm}{sec}\ \frac{ft}{(12)2.54\ cm} \times$

$\times\ [(95)\ 0.239\ \frac{Btu}{\#\ ^oR}]$

$= 4.69 \times 10^5\ \frac{Btu}{hr\ ft^2 {}^oR}$

with $C_{p_{10,800\ ^oR}} = 95\ C_{p_{560\ ^oR}}$

from Fig. 11.15 Rohsenow and Choi[58]

The time required to raise the Cu sphere from its melting point (1356 ^{o}K) to its boiling point (2868 ^{o}K) can be calculated in the following way:

If the internal resistance of the sphere is negligible compared to the external resistance, the temperature (T) of the sphere at time (t) is given by (see Kreith[59])

$$\frac{T - T_\infty}{T_o - T_\infty} = e^{-(Bi)(9k_s t/\rho c r^2)}$$

where $Bi = \frac{hV}{k_s A_s} = \frac{h\,r}{k_s\,3}$.

If Bi < 1 the internal resistance is neglibible.

$$Bi = \frac{h\,r}{3\,k_s} = \frac{4.69 \times 10^5}{3(207)} \quad \frac{0.001}{2(12)} = .0315 < 1$$

$$\therefore \quad \frac{2868 - 6000}{1356 - 6000} = 3^{-(.0315)\left[\frac{9(207) \quad 4(144) \quad t}{558\ (.091)(.001)^2(3600)}\right]}$$

$$\therefore \quad t = 2.1 \times 10^{-6} \text{ sec.}$$

Therefore, the heating effect of the gas jet is significant. The gas jet can heat up molten copper spheres, as large as 0.001" in diameter, to their boiling temperature. And this heating takes place in less time than it takes for the sphere to traverse the gap (i.e., 2 μ sec. < 19 μ sec).

4.1.5 Improvement of EDM Realizing the Presence of Gas Jets

From the previous analysis, it can be concluded that increasing the gap distance will increase the effectiveness of Maecker's gas jets. Increasing the gap distance will allow the gas jets to be better formed and to increase the plating on the anode. The following suggests three possible ways of causing the arc to breakdown at larger gap spacings. The obvious solution is to increase the voltage supplied to the gap. Another means of increasing the gap distance is to use a liquid dielectric with a lower breakdown strength. The third possibility to achieve a larger gap spacing is to dope the liquid dielectric with particles that would reduce the dielectric strength of the mixture. These possibilities are suggested for future investigations. Thus it may be possible to achieve negligible erosion of the anode tool at high machining frequencies. This is desirable so that a better surface finish is obtained without tool erosion.

4.2 Liquid Metal Removal from Electrodes

Although the above theory using Maecker's gas jets does describe how liquid metal is propelled, it does not tell how the liquid metal is initially ejected from the electrode. We believe that this question of how the liquid metal is removed from the surface is very important to the understanding of EDM.

The belief that liquid metal removal is important is substantiated by the presence of large particles in the liquid dielectric after machining. A good percentage of these particles are hollow spheres which can be caused by the solidification of molten metal.[1,4]

The two conflicting theories presented below illustrate that the mechanism of liquid metal removal from the electrodes has not been fully established. Zolotykh, Gioyev, and Tarasov[60] say that they observed an expanding bubble during the discharge using high-speed photography. Then when the discharge is shut off, the bubble keeps on expanding, thus causing a reduction in the pressure above the molten pool at the anode spot. When the pressure decreases to below atmospheric pressure, Zolotykh et al. say that the molten metal is boiled off. They state that this boiling off at the termination of the discharge accounts for 85% of the erosion of the electrode.

The second theory of liquid metal removal is presented by Zingerman[61]. He observes metal particles being ejected from the anode spot during the discharge, which contradicts the observations of Zolotykh et al. Zingerman states that the data of Zolotykh et al. lack sufficient reliability. Because their data referred to the formation of pits at the edge of thin electrodes 0.1 mm thick and edge mounted, Zingerman says that the liquid metal mainly ran off the edge of the electrode. Since the molten metal is seen being ejected during the discharge, Zingerman puts forth the following hypothesis of the ejection mechanism, although he does not substantiate this hypothesis. "It may be assumed that the ejection of metal proceeds as the results of vaporization of internal small regions located below the surface of the electrode. Such a process results from the presence of nonuniformities with various thermophysical properties which determine nonmonotomic distribution of the temperature field."

The contradictions between the observations of these two papers may be settled if the timesof the discharge pulses are analyzed. The discharges used by Zingerman last for times greater than 7 msec, and he says that metal vapor appears within 0.1 msec after the beginning of the discharge. Since Zolotykh et al.'s greatest arc duration was 0.18 msec, it may mean that two different methanisms occur between arcs of duration less than 0.18 msec and arcs of duration greater than 7 msec.

4.3 Erosion Jets Occurring in Other Discharges

Below are four cases where eroded material is given off from a surface. By observing erosion jets or flares occurring in other conditions other than EDM, it is hoped to better understand the gas jets and erosion phenomenon that are observed in EDM.

4.3.1 Crystal Growing in an Arc Discharge

An outstanding example of metal transfer from the cathode to the anode is seen in growing crystals in an arc discharge. Drabble and Palmer[62] describe this process using a 2 to 20 amp continuous discharge in air. Using a seed crystal as the anode, cathode material is built upon this seed to form a single crystal.

4.3.1.1 Crystal Growing Used in Understanding EDM

Drabble and Palmer's[62] description of crystal growing using an arc, vividly illustrates that the net transfer of material during the arc is from the cathode to the anode. This agrees with our observations of cathode metal being plated on the anode in EDM. Our understanding of EDM may also be increased further when more is learned about the above method of growing crystals.

4.3.2 Nanosecond Arcs

Vapor jets have also been observed in nanosecond arc discharges. Using a 4000 amp, 20 nsec arc discharge in air, Fischer and Gallagher[63] observed anode vapor jets. During the discharge, they photographed an expanding luminous bubble from the anode. After the current is cut off, jet-like flares seem to grow from the Cu anode. Time-resolved spectroscopy indicates no trace of the Cu spectrum at the anode which Fischer and Gallagher say is understandable if the jets are made up of large anode particles. This condition prevails if the afterglow channel does not have adequate thermal energy to vaporize these large particles.

At current cut-off Fischer and Gallagher[63] also observe a shock wave from the cathode which confirms Sigmond's[64] theory of the release of a high-pressure ion sheath at the cathode.

By spectroscopic measurements, Sigmond[64] follows a shock wave of tungsten cathode vapor across the arc after the current is cut off. The velocity of the shock wave was determined to be 2×10^6 cm/sec for a 30 amp, 30 nsec arc in hydrogen of 2 atm pressure. Tungsten vapor was also observed during the discharge (after a few nsec) at the cathode. Sigmond observed an increase in intensity of the tungsten vapor by spectroscopic measurements at the end of the pulse. The progress of the tungsten vapor across the gap (0.20 mm) can also be seen in Sigmond's spectroscopic measurement.

4.3.2.1 Nanosecond Arcs Used in Understanding EDM

Two major points that we have derived by studying nanosecond arcs are the following: First, we realize that a refractory cathode

can be heated up significantly with the high current density present in the spark phase of an arc. This point will be discussed in more detail in Appendix B. The second observation derived from Fischer and Gallagher's work is the erosion of the anode in the nanosecond range. This anode erosion has been previously stated in Section 3.2.3.1.

4.3.3 Vacuum Arcs

By the very nature of vacuum arcs, there must be erosion of at least one of the electrodes in order for the arc to exist. A good description of vacuum arcs is given by Cobine and Vanderslice[65]. They state that, "The cathode spots of the vacuum arc are essentially the same in appearance as seen on surface mercury pool tubes and on cold metals at high pressures." "In vacuum the high density vapor at the cathode spot diffuses rapidly away to a low value, probably of the order of that corresponding to 1 - 30 x 10^{-3} mm Hg. The column is therefore diffuse, as photographs and visual observations reveal. A concentrated column and anode spots can only occur at high currents (> 300 amps) where the instantaneous vapor density in the gap becomes very high, and the confining effects of the self-magnetic field becomes important." "However, at high currents anode spots with characteristic molten areas appear."

Since most of the erosion in vacuum arcs occurs at the cathode, the vapor jets observed are from the cathode. Von Engel and Arnold[66] measured the velocity distribution of the cathode vapor jet and found the average velocity of neutral particles to be 4 x 10^{4} cm/sec. Davis

and Miller[67,68] determined that the amount of neutral cathode particles eroded increased almost linearly with current. These two men also found that the majority of the ions given off by the arc have energies greater than the arc voltage. One explanation of these high energies is the presence of a potential peak near the cathode.

4.3.3.1 Vacuum Arcs Used in Understanding EDM

In studying vacuum arcs we notice that the same type of jet is observed emanating from the cathode as was observed by Maecker. The similarities are in the fact that the jet is from the cathode and that its velocity is approximately the same in both cases.

In the vacuum arc, at low currents, there is erosion of the cathode but no erosion of the anode. This contrasts with the anode erosion observed in EDM. Because of the diffuse nature of a vacuum arc (actually a low-pressure arc), this difference could be explained as follows: In a low-pressure arc the arc diffuses rapidly from the cathode, thereby producing a very low current density at the anode. Since the cathode erosion increases with current, anode erosion is observed at high currents. This anode erosion occurs because the increased cathode erosion produces a high instantaneous vapor density which gives an effective high-pressure arc. This effective high-pressure arc is similar to our EDM arc; therefore, anode erosion is observed.

4.3.4 Lasers

Jets of eroded metal are observed for laser irradiated surfaces. Since there are two types of lasers, the following descriptions of

them will be given first. The first laser, which Ready[69] calls the ordinary laser, lasts for several hundred μsec, although it has oscillating spikes of about μsec duration and has energy densities of 10^6 to 10^7 watts/cm^2.

The jets of vapor observed for these ordinary lasers are suggested by Ready to arise from continuous evaporization of the surface. The second type of laser is called a Q-switch laser and has energy densities of 10^7 to 10^9 watts/cm^2. The Q-switch laser produces a much higher energy density than the ordinary laser, but only has a duration of several tens of nsec. The jet of material given off by a Q-switch laser does not occur until after the laser pulse has ended ($\sim$ 120 nsec after pulse). Ready suggests that a superheated region is formed beneath the surface which explodes after the pulse has ended.

4.3.4.1 Lasers Used in Understanding EDM

In the future it may be possible to observe the erosion produced by lasers in understanding EDM. Lasers would be advantageous to use for studying the erosion of a single electrode because the effect of the other electrode and the small gap space can be eliminated. But, at the present development of lasers, the oscillations in the ordinary lasers and the enormously high energy densities in the Q-switch laser seem to prohibit the simulation of an arc by a laser.

4.4 Conclusions from Gas and Erosion Jets

The cause of the apparent reduced anode erosion can be explained by the plating of cathode metal on the anode. Thus the cathode metal plating on the anode protects the anode from further erosion.

In the preceding analysis Maecker's gas jets were shown to be capable of propelling cathode metal to the anode at large gap distances. Along with the quantitative results, Maecker's experiments vividly illustrate the power of the gas jet. He did this by observing carbon particles interjected at the cathode being propelled to the anode.

Because of the present lack of sufficient experimental evidence, it cannot be stated conclusively that Maecker's gas jets are the total mechanism for anode plating. But, it can be said that the gas jet's increase in strength occurs when increased plating is present.

5.0 CONCLUSIONS

The following conclusions describe the EDM erosion phenomenon in terms of the energy balance analysis of the two modes of EDM (i.e., I,Standard,and II, Reverse Polarity). The conclusions also describe spark erosion and electrode plating which are the two additional factors necessary for understanding the erosion mechanism.

I. Standard Polarity

Until recently, the more conventional mode of using an EDM machine was to operate with the workpiece as the anode and the tool as the cathode (called standard polarity). Under these conditions most of the erosion occurred on the anode; however, there also was always a significant amount of erosion of the cathode. Most of the previous work done in investigating EDM was accomplished by empirical techniques. Usually just machining rates were measured when different tool materials and liquid dielectrics were tried. Copper and graphite were found to be good tool materials for machining steel.

The approach used in this investigation, of analyzing the erosion mechanism in EDM in terms of the electrical discharge that occurs, was highly successful in explaining the above conditions. Also, all of the conclusions drawn are consistent with experiments done with a single discharge apparatus and an Elox EDM machine, although these conclusions cannot be said to have been experimentally proven because the number of tests that have been run is limited. In order to use an arc discharge analysis, the electrical discharge occurring in EDM was shown to possess the same characteristics as a high pressure

(1 atmosphere) arc discharge in air. For clarity the results of the arc energy balance analysis are described below in terms of a copper and a carbon tool separately.

a. Copper Cathode Tool - Steel Anode Workpiece

Using a copper cathode and a steel anode, it was determined that the percentages of total arc energy transferred to the anode and cathode were approximately 70 percent and 7 percent, respectively. With this energy distribution, and because the energy densities to the cathode and anode were found to be of the same order of magnitude, it is concluded that the steel anode should erode ten times as much as the copper cathode, since copper and steel are thermally similar. It should be emphasized that this result is consistent with the choice of using the tool as the cathode as is done in standard polarity. This prediction also is supported by our experimental data indicating that the erosion of a steel anode is several times greater than of a copper cathode for the usual standard polarity condition of gap spacings $\cong$ 0.001". Unfortunately the total amount of metal eroded cannot be accounted for as successfully as the relative erosion between the cathode and anode. A straightforward calculation proves that only 5% of the total arc power is needed to melt the observed amount of eroded metal. The rest of the arc power may qualitatively be accounted for by the power associated with vaporization and incomplete removal of molten metal.

The validity of using the energy balance analysis to explain erosion for the arc durations encountered in EDM (4 μs to 5 x 10^3 μs)

was substantiated by determining the times required to raise copper and steel up to their melting points (approximately 11 μs and 2 μs, respectively).

b. Carbon Cathode Tool - Steel Anode Workpiece

When carbon (graphite) is used as the cathode, the energy balance analysis also predicts that the percentage of arc energy to the steel anode and to the carbon cathode will be approximately 70 percent and 7 percent, respectively. But it was determined that it was not valid to use the arc energy balance analysis to explain erosion for the arc durations encountered in EDM, because these discharge times (4 μs to 5 x 10^3 μs) were less than the time (∿ 3 sec) needed to raise the carbon and the steel up to their melting points. The enormous differences between the times needed to raise the electrodes up to their melting points using a carbon cathode (∿ 3 sec) as compared to when a copper cathode (2 and 11 μs) is used results from the energy density produced by a copper cathode being ∿ 10^3 times greater than that produced by a carbon cathode. This difference in energy densities occurs because the arc current density of a low melting point cathode (i.e., copper) is ∿ 10^3 times greater than the arc current density of a refractory cathode (i.e., carbon).

The mechanism that was found to explain the observed EDM erosion using a carbon cathode (since it could not be described with the energy balance analysis for the carbon arc discharge) was spark erosion. This conclusion was supported by experimental data for single-arc discharges that indicate that the amount of erosion from an

anode* was approximately independent of the arc duration in the range 13 μ sec to ∿ 3 sec.

II. Reverse Polarity

Recently a mode of machining has been discovered (called reverse polarity) that seems completely contradictory to the above-described mode. The apparent contradiction arises because even though copper and carbon are still used to machine steel, the polarities are inverted, the workpiece now being the cathode.

When reverse polarity is used, the anode erosion is almost always less than the cathode erosion, and, under certain conditions of large gap distances, there is no anode erosion. This unexpected decrease in anode erosion for reverse polarity is described below for the two tool materials, copper and carbon.

a. Copper Anode Tool - Steel Cathode Workpiece

Since the energy balance analysis supported the choice of the workpiece being the anode for standard polarity, by predicting ten times the amount of anode erosion as cathode erosion, it could not possibly justify using the workpiece as the cathode in reverse polarity. But the reduction in anode erosion when reverse polarity conditions are used can be explained by observations of cathode metal being plated on the anode. Thus, it is proposed that this plating protects the anode because the plating has to be eroded before the arc can reach the original anode metal. The reason that this plating on the anode

---

*Although this test was run with a copper anode, it is believed that the results would be the same for steel since steel is thermally similar to copper.

usually occurs in reverse polarity and not in standard polarity is only because larger gap distances are normally used in reverse polarity. (Actually plating has been observed by T. Viswanathan[6] in standard polarity if large gap distances are used.)

It is proposed that this plating is caused by gas jets being formed at large gap distances (0.005" to 0.007") propelling cathode metal, in its vapor and molten state, to the anode. Maecker has photographed these gas jets and described them as resulting from the arc's magnetic field. In fact, calculations show that these gas jets are capable of carrying cathode material across the electrode gap to the anode.

b. Carbon Anode Tool - Steel Cathode Workpiece

The explanation of why carbon is used as the anode in reverse polarity is the same as was given above for copper. An advantage that can be noted for carbon is that it normally erodes much less than copper; therefore, less protection is needed from the plating of the cathode metal.

6.0 RECOMMENDATIONS FOR FUTURE WORKS

In general many more experiments are needed (including variations of electrode metals, dielectric current, gap spacing, and arc duration) to verify the conclusions drawn in this thesis, which are briefly:

a. The amount of arc energy delivered to the anode and cathode are 70 percent and 7 percent, respectively.

b. Spark erosion occurs when a refractory cathode is used; whereas, using a low melting point cathode, the erosion is caused by the arc.

c. Plating of cathode metal on the anode is accomplished at large gap distances and can be explained by Maecker's gas jets.

Suggested experiments that should aid to the verification of the conclusions are listed below:

1. More experiments can be done with similar low melting point electrodes (Cu, Fe, Al, Sn) to verify that the amount of energy delivered to each electrode is the same as indicated above.

2. One test which can be performed to help verify that spark erosion occurs when a refractory cathode is used is to try another refractory metal (other than carbon) as the cathode. Tungsten might be suitable since it would not be eroded mechanically as in the case of graphite.

3. Since spark erosion has been observed for refractory cathodes, it may also be present when a low melting point cathode is used; therefore, it is suggested that this possibility be investigated

by extending the range of the single-discharge apparatus from 13 μs down to 1 μs to analyze the spark.

4. Taking fast (∿ μ sec) photographs of the arc discharge on the single-discharge apparatus may aid in determining when and by what means molten metal is ejected from the electrodes. This knowledge would verify the conditions under which the plating of the cathode metal onto the anode occurs. Also, the possibility of learning how the molten metal is ejected from the electrodes should be emphasized, since it is fundamental to the complete understanding of the EDM process.
5. Another technique that could prove useful in studying the plating of cathode metal onto the anode is to use an irradiated cathode. Then the amount of cathode metal and its distribution on the anode could be analyzed.
6. For reasons given in Chapter 4, we believe that the condition of cathode metal being plated on the anode is primarily dependent upon large gap distances. However, this dependence has not been absolutely established for EDM machines because the gap distance is dependent upon the energy delivered per pulse. Thus a critical test that could be performed on the EDM machine is to machine at large gap distances while varying the amount of energy discharged per pulse. This condition was also suggested in Section 4.1.5 as the method to improve EDM.

REFERENCES

1. P. E. Berghausen, H. D. Brettschneider, and M. F. Davis, "Electro-Discharge Machining Process," Technical Documentary Report No. ASD-TDR-7-545 of the Cincinnati Milling Machine Co., Ohio, 1963.
2. M. M. Barash, Ph.D. thesis, Victoria University of Manchester (1958).
3. Stanley A. Doret, "An Experimental Investigation of EDM Using A Single Pulse Technique," Master's Thesis, M. E. Dept., M.I.T., January 1968.
4. H. C. Juvkam-Wold, "An Experimental Investigation of EDM Using Reverse Polarity," Master's Thesis, M. E. Dept., M.I.T., August, 1967.
5. H. C. Juvkam-Wold, Work currently being done for Ph.D. Thesis, M. E. Dept., M.I.T.
6. T. Viswanathan, Work currently being done for Ph.D. Thesis, M. E. Dept., M.I.T.
7. J. M. Somerville, W. R. Blevin, and N. H. Fletcher, Proc. Phys. Soc., B65, 963 (1952).
8. J. M. Somerville, The Electric Arc, Methuen Physical Monograph, (Butler and Tanner, Ltd., Frome and London, Great Britain, 1959) p. 5.
9. W. R. Blevin, Austr. J. Sci. 6, 203 (1953).
10. See p. 89 in Ref. 8.
11. A. Von Engel, Ionized Gases, (Oxford Univ. Press, 2nd Ed., 1965) p. 275.

12. G. Busz-Peuckert and W. Finkelnburg, Z. Physik, 140, 540, (1955). (In German).

13. G. Busz-Peuckert and W. Finkelnburg, Z. Physik, 144, 244, (1956). (In German).

14. K. D. Froome, Pro. Phys. Soc. 60, 424 (1948).

15. K. D. Froome, Brit. J. Appl. Phys., 4, 91 (1953).

16. K. D. Froome, Proc. Phys. Soc. B62, 805 (1949).

17. J. D. Cobine and C. J. Gallagher, Phys. Rev. 74, 1524 (1948).

18. M. J. Druyvestyn and F. M. Penning, Revs. Mod. Phys. 12, 87 (1940).

19. See p. 123 in Ref. 8.

20. See p. 64 in Ref. 8.

21. A. Von Engel and K. W. Arnold, Proc. Phys. Soc. 79, 1098 (1962).

22. J. D. Cobine, Gaseous Conductors, (Dover Publications, Inc., New York, 1958, 2nd ed.) p. 109.

23. See p. 89 in Ref. 8.

24. J. D. Cobine and E. E. Burger, J. Appl. Phys. 26, 895 (1955).

25. See p. 88 in Ref. 8.

26. See p. 90 in Ref. 8

27. W. Bez and K. H. Hocker, Z. Naturf. 11a, 118, (1956). (In German).

28. See p. 281 in Ref. 11.

29. W. Elenbaas, The High Pressure Mercury Vapour Discharge, (Interscience Publishers, Inc., New York, 1951), p. 144.

30. F. Llewellyn Jones, Brit. J. Appl. Phys. 1, 60 (1950).

31. See p. 6 in Ref. 8.

32. C. G. Suits, Physics 6, 315 (1935).

33. See p. 30 in Ref. 8.

34. See p. 11 in Ref. 29.

35. See p. 62 in Ref. 8.

36. F. Llewellyn Jones, The Physics of Electrical Contacts, (Oxford Univ. Press, 1957),p. 165.

37. L. H. Germer and W. S. Boyle, J. Appl. Phys. 27, 32, (1956).

38. M. M. Barash and C. S. Kahlon, Int. J. Mach. Tool Des. Res., 4, 1, (1964).

39. S. S. Mackeown, Phys. Rev. 34, 611 (1929).

40. See p. 75 in Ref. 8.

41. See p. 68 in Ref. 8.

42. A. Von Engel and A. E. Robson, Proc. Roy. Soc. A242, 217 (1957).

43. See p. 76 in Ref. 8.

44. See p. 71 in Ref. 8.

45. R. H. Eather, Austr. J. Phys. 15, 289, (1962).

46. J. Rothstein, Phys. Rev., 73, 1214, (1948).

47. A. M. Cassie, Nature, 181, 476,(1958).

48. J. M. Somerville and C. T. Grainger, Brit. J. App. Phys. 7, 109, (1956).

49. C. T. Grainger, M. Sc. Thesis, Univ. of New England, (1956).

50. See p. 20 in Ref. 8.

51. I. G. Kesaev, Soviet Physics-Technical Physics, 9, 1146, (1965).

52. See p. 66 in Ref. 8.

53. W. Finkelnburg, Phys. Rev. 74, 1975 (1948).

54. See p. 102 in Ref. 8.

55. H. Maecker, Z. Phys. 141, 198 (1955). (In German) Translated by Associated Technical Services, Inc., New Jersey, No. 07G6G.

56. See p. 95 in Ref. 8.

57. S. L. Mandel'shtam and S. M. Raiskii, Izvestiya Akademii Nauk SSSR, Ser. Fiz., Vol. 13, 1949, No. 5, pages 549-565. (Henry Brutcher, Altadena Calif. translation No. 2526).

58. W. M. Rohsenow and H. Choi, Heat, Mass and Momentum Transfer (Prentice-Hall, Inc., New Jersey, 1961) Chap. 11.

59. F. Kreith, Principles of Heat Transfer, (International Textbook Co., Scranton, Penn., 1958) p. 135.

60. B. N. Zolotykh, K. Kh. Gioyev, and Ye. A. Tarasov, Problemy Elektricheskoy Obrabotki Materialov, 1960, pp. 58-64.

61. A. S. Zingerman, Izvestiya Vysshikh Uchebnykh Zavedenity, Fizika., No. 1, pp. 21-30, (1963) (Translation FTD-TT-69-950/1 + 2).

62. J. R. Drabble and A. W. Palmer, J. Appl. Phys., 37, 1778, (1966).

63. H. Fischer and C. C. Gallagher, Report on 26th Annual Conference Physical Electronics, 385 (1966), M.I.T., Cambridge, Mass.

64. R. S. Sigmond, Proc. Phys. Soc., 85, 1269 (1965).

65. J. D. Cobine and T. A. Vanderslice, Communication and Electronics, IEEE, May 1963.

66. A. Von Engel and K. W. Arnold, Phys. Rev. 125, 803 (1962).

67. W. D. Davis and H. C. Miller, General Physics Research Report No. 65-C-050 (1965), General Electric R and D Center, Schenectady, New York.

68. W. D. Davis and H. C. Miller, General Physics Laboratory Report No. 66-C-378, General Electric (R and D Center, Schenectady, New York).

69. J. F. Ready, J. Appl. Phys., 36, 462, (1965).

APPENDIX A

DERIVATION OF MAECKER'S GAS JET THEORY

A.1

The following solutions are given by Maecker[55] to determine the maximum magnetic pressure, P_{max}, the maximum velocity of the gas stream, v_{max}, and the recoil force, F_c, on the cathode. The forces acting at the constriction in front of the cathode are shown below.

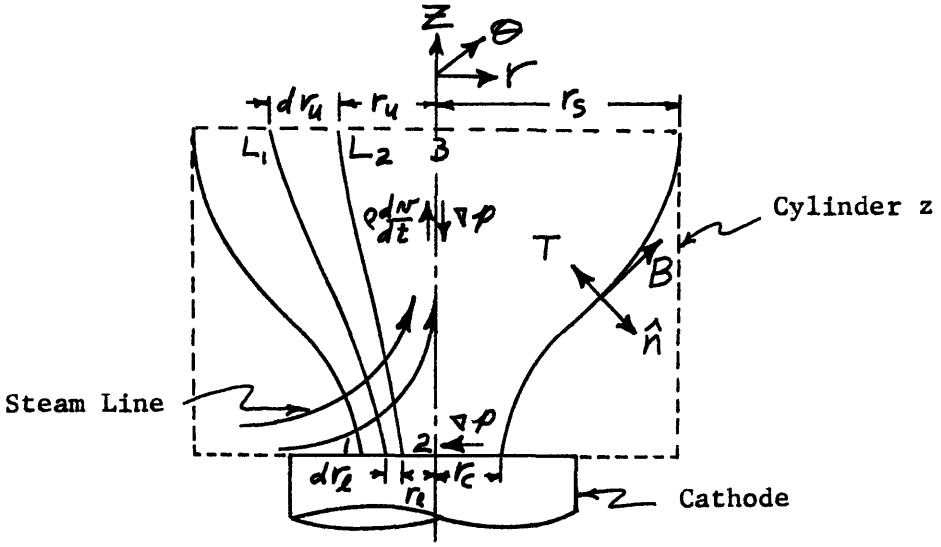

The equation of motion for the arc is stated as

$$\rho \frac{D\bar{v}}{Dt} = (\bar{J} \times \bar{B}) - \nabla p$$

where $(\bar{J} \times \bar{B})$ is the Lorentz force caused by the self-magnetic field of the arc;

∇p is the pressure gradient;

$\rho \frac{D\bar{v}}{Dt}$ is the mass density times the acceleration of the gas stream.

A.2 Maximum Pressure

By neglecting the mass flow, $\frac{D\bar{v}}{Dt} = 0$, the maximum pressure in the center of the arc can be calculated. The condition can exist directly

in front of the cathode (see figure above) before the gas stream is developed.

$$0 = (\bar{J} \times \bar{B}) - \nabla p$$

$$\nabla p = \frac{\partial p}{\partial r} \hat{u}_r + \frac{1}{r} \frac{\partial p}{\partial \theta} \hat{u}_\theta + \frac{\partial p}{\partial z} \hat{u}_z$$

Considering the radial direction only

$$\nabla p = \frac{\partial p}{\partial r} \hat{u}_r$$

$$\bar{J} \times \bar{B} = \begin{vmatrix} \hat{u}_r & \hat{u}_\theta & \hat{u}_z \\ J_r & J_\theta & J_z \\ B_r & B_\theta & B_z \end{vmatrix}$$

$$= \hat{u}_r (J_\theta B_z - J_z B_\theta) - \hat{u}_\theta (J_r B_z - J_z B_r) + \hat{u}_z (J_r B_\theta - J_z B_r)$$

$\bar{J} \times \bar{B} = -J_z B_\theta \hat{u}_r$ because the magnetic field is in the θ-direction only, and the current density is in the z-direction only; therefore,

$$\frac{dp}{dr} = -J_z B_\theta$$

Before integrating dp, an expression for B_θ will be derived using the relationship that the curl of the magnetic field strength equals μ_o times the current density

$$\nabla \times \bar{B} = \mu_o \bar{J}$$

$$\nabla \times \bar{B} = \frac{1}{r} \begin{vmatrix} \hat{u}_r & r\hat{u}_\theta & \hat{u}_z \\ \frac{\partial}{\partial r} & \frac{\partial}{\partial \theta} & \frac{\partial}{\partial z} \\ B_r & rB_\theta & B_z \end{vmatrix}$$

$$= \frac{1}{r}\left\{ \hat{u}_r\left[\frac{\partial B_z}{\partial \theta} - \frac{\partial (rB_\theta)}{\partial z}\right] - r\hat{u}_\theta\left[\frac{\partial B_z}{\partial r} - \frac{\partial B_r}{\partial z}\right] + \hat{u}_z\left[\frac{\partial (rB_\theta)}{\partial r} - \frac{\partial B_r}{\partial \theta}\right]\right\}$$

$$= \frac{1}{r}\frac{\partial (rB_\theta)}{\partial r}\hat{u}_z \qquad \text{using} \quad \begin{cases} \bar{B} = B_\theta \\ \dfrac{\partial (rB_\theta)}{\partial z} = 0 \end{cases}$$

Since $\bar{J} = J_z$ only

$$\mu_o J_z = \frac{1}{r}\frac{\partial (rB_\theta)}{\partial r}\hat{u}_z$$

or $$B_\theta = \frac{\mu_o}{r}\int_o^r J_z\, r\, dr$$

Using this expression for B_θ in the above equation for $\frac{dp}{dr}$, one obtains the following:

$$dp = -\mu_o \frac{J_z}{r}\int_o^r J_z\, r\, dr$$

integrating

$$\int_{p_o}^{p_r} dp = -\mu_o \int_o^r \frac{J_z}{r}\int_o^r J_z\, r\, dr\, dr$$

The assumption is made that the current density is uniform over the cross section of the arc. This is a fair assumption since the current density does fall off very sharply in an arc according to the Saha equation (see Chapter 2, Section 2.2.6).

$$p_r - p_0 = -\mu_0 J_z^2 \int_0^r \frac{r}{2}\, dr$$

$$= -\frac{\mu_0}{4} J_z^2 r^2$$

$$p_0 - p_r = \frac{\mu_0 J_z^2 r^2}{4}$$

Let $p_r = p_{r_c}$ = atmospheric pressure; then the gage pressure at the center of the arc equals the maximum value

$$p_{max} = \frac{\mu_0 J_z^2 r_c^2}{4}$$

with $J_z = \frac{I}{\pi r_c^2}$ I = total current

p_{max} also equals $\frac{\mu_0 J_z I}{4\pi}$ or $\frac{\mu_0 I^2}{4\pi^2 r_c^2}$

Maecker determines the maximum pressure at the cathode for a carbon cathode with a current of 200 amps to be about 7 mm Hg.

$$p_{max} = \frac{\mu_o I J}{4\pi}$$

where I = arc current = 200 amp

J = current density

$$= \frac{I}{\pi r_c^2} = \frac{200 \text{ amp}}{\pi (.12 \text{ cm})^2} = 4400 \text{ amp/cm}^2$$

$$= 4.4 \times 10^7 \text{ amp/m}^2$$

μ_o = permeability of free space

$$= 4\pi \times 10^{-7} \text{ nt/amp}^2$$

p_{max} = pressure in nt/m^2

(1 atm = 10^5 nt/m^2)

$$p_{max} = \frac{4\pi \times 10^{-7} \text{ nt/amp}^2 \; 200 \text{ amp} \; 4.4 \times 10^7 \text{ amp/m}^2}{4\pi}$$

$$\cong 900 \text{ nt/m}^2 \cong 7 \text{ mm Hg}$$

Comparing this value of 7 mm Hg to 0.6 mm Hg, which is the pressure calculated in the column of the arc with a radius of .4 cm, illustrates that the pressure gradient is directed away from the cathode.

For low melting point cathodes with current densities greater than 10^6 amp/cm^2 (see Section 2.2.2), the maximum pressure would achieve values above 1670 mm Hg for 200 amp.

In order to measure the maximum pressure, a small axial hole of radius r_i can be put in the cathode for use with a water manometer. If the current density is assumed to be the same as without a hole, the radius of the cathode spot, r_b, will increase, thus causing the magnetic field to decrease. The maximum pressure will then decrease in the following way:

Changing the limits on

$$\int_{p_o}^{p_r} dp = -\mu_o \int_0^r \frac{J_z}{r} \int_0^r J_z r\,dr\,dr$$

to

$$\int_{p_i}^{p_r} dp = -\mu_o \int_{r_i}^r \frac{J_z}{r} \int_{r_i}^r J_z r\,dr\,dr$$

$$p_r - p_i = -\frac{\mu_o J_z^2}{4}\left[r^2 - r_i^2 - 2r_i^2 \ln \frac{r}{r_i}\right]$$

with $$J_z = \frac{I}{\pi r_b^2 - \pi r_i^2}$$

$$p_{max} = p_i - p_{r=r_b}$$

$$= \frac{\mu_o I J_z}{4(\pi r_b^2 - \pi r_i^2)}\left[r_b^2 - r_i^2 - 2r_i \ln \frac{r_b}{r_i}\right]$$

using $\pi r_c^2 = \pi r_b^2 - \pi r_i^2$

$$p_{max} = \frac{\mu_0 I J_z}{4\pi}\left[1 - 2\left(\frac{r_i}{r_c}\right)^2 \ln\left(1+\frac{r_c^2}{r_b^2}\right)\right]$$

A.3 Maximum Velocity of Gas Stream

The equation of motion, $\rho \frac{D\bar{v}}{Dt} = (\bar{J} \times \bar{B}) - \nabla p$, will now be used to calculate the maximum velocity that the gas stream could reach. The continuity equation, $\frac{\partial \rho}{\partial t} + \nabla \cdot (\rho \bar{v}) = 0$, will also be used in this analysis. If a steady flow is assumed, these two equations may be reduced as follows:

$$\frac{D\bar{v}}{Dt} = \frac{\partial \bar{v}}{\partial t} + (\bar{v}\cdot\nabla)\bar{v}$$

$$= (\bar{v}\cdot\nabla)\bar{v}$$

$$\frac{\partial \rho}{\partial t} + \nabla\cdot(\rho\bar{v}) = \nabla\cdot(\rho\bar{v}) = 0 \;;$$

therefore,

$$\bar{J}\times\bar{B} = \nabla p + \rho(\bar{v}\cdot\nabla)\bar{v}$$
$$\nabla\cdot(\rho\bar{v}) = 0$$

Using the vector identity $\nabla(\bar{v}\cdot\bar{v}) = 2(\bar{v}\cdot\nabla)\bar{v} + 2\bar{v}\times(\nabla\times\bar{v})$, $(\bar{v}\cdot\nabla)\bar{v}$ may be reduced to $\frac{\nabla v^2}{2}$ when integrating along a streamline.

Integrating the equation of motion along a streamline (see figure above), an analogous equation to the Bernoulli equation is obtained.

$$\int (\bar{J} \times \bar{B}) \cdot d\bar{s} = \int \nabla p \cdot d\bar{s} + \int \rho \nabla \frac{v^2}{2} \cdot ds$$

$$\int (\bar{J} \times \bar{B}) \cdot ds = p \Big|_{p_{a=1}}^{p_{b=2}} + \rho \frac{v^2}{2} \Big|_{v_{a=1}}^{v_{b=2}}$$

If this integration is done along the streamline that leads up to the axis of the arc at the cathode (point 1 to 2 of figure above), the velocity disappears according to the continuity equation. Thus the Lorentz force equals the pressure gradient which was used in Section A3.2 to calculate the maximum pressure.

Since there are no Lorentz forces acting along the axis of the arc (point 2 to 3 of figure), the integrated equation of motion is

$$p_3 - p_2 = -\rho \left(\frac{v_3^2 - v_2^2}{2} \right) .$$

With $v_2 = 0$ and $p_3 = 0$, the maximum velocity that the gas stream could reach would be $v_{max} = \sqrt{\frac{2 p_2}{\rho}}$

Setting $p_2 = p_{max}$ (the maximum pressure attainable at the cathode), the maximum velocity equals

$$v_{max} = \sqrt{\frac{2 p_{max}}{\rho}}$$

for $p_{max} =$ 900 nt/m^2 (7 mm Hg) and $\rho = 1.5 \times 10^{-5}$ gm/cm^3, Maecker obtains a maximum velocity of 3.5×10^4 cm/sec.

$$v_{max} = \sqrt{\frac{2 \left(900 \frac{kg\,m}{sec^2 m^2}\right) 10^3 gm\, m}{1.5 \times 10^{-5} \frac{gm}{cm^3}\, kg\, 10^2 cm}}$$

$$\cong 3.5 \times 10^4 \ cm/sec$$

A.4 Recoil Force on the Cathode

The recoil force on the cathode equals the momentum generated in the arc, which can be expressed as the volume integral of the acceleration term $\rho(\bar{v}\cdot\nabla)\bar{v}$ in the equation of motion. The force, F_c, therefore equals

$$F_c = \int_V \rho(\bar{v}\cdot\nabla)\bar{v}\,d\tau = \int_V (\bar{J}\times\bar{B})\,d\tau - \int_V \nabla p\,d\tau$$

The volume integral of the Lorentz force, $\int(\bar{J} \times \bar{B})d\tau$, can be treated in terms of Maxwell's stresses, $\bar{T}$.

$$\int_V (\bar{J}\times\bar{B})\,d\tau = \oint_S \bar{T}\,ds$$

where $\bar{T} = \bar{B}(\hat{n}\cdot\bar{H}) - \frac{1}{2}\hat{n}(\bar{B}\cdot\bar{H})$;

$\bar{H}$ = magnetizing field = $\frac{\bar{B}}{\mu_0}$ for air;

$\hat{n}$ = unit normal vector to surface area dS.

The magnitude of $\bar{T}$ is given by

$$|\bar{T}| = \frac{1}{2}\bar{B}\cdot\bar{H} = \frac{1}{2\mu_0}B^2 \text{ for air,}$$

and its direction is such that $\bar{B}$ bisects the angle between $\bar{T}$ and the normal vector, $\hat{n}$. Maecker circumscribes the arc at the cathode with a cyliner z (see figure above) in order to analyze the stresses. The stresses can be calculated by using the expression for the magnetic field strength in the Θ-direction calculated previously.

$$B_\Theta = \frac{\mu_0}{r}\int_0^r J_z\,r\,dr;$$

therefore,

$$|\bar{T}| = \frac{1}{2\mu_0} B^2$$

$$= \frac{\mu_0}{2r^2}\left[\int_0^r J_z\, r\, dr\right]^2 .$$

But since

$$I = 2\pi \int_0^r J_z\, r\, dr$$

$$|\bar{T}| = \frac{\mu_0 I^2}{8\pi^2 r^2}$$

The force $\bar{T}\, dS_u$ acting on the upper part of cylinder z between the current paths L_1 and L_2 (see figure above) is

$$\bar{T}\, dS_u = \frac{\mu_0 I_r^2}{8\pi^2 r_u^2} 2\pi r_u\, dr_u$$

$$= \frac{\mu_0 I_r^2}{4\pi} d(\ln r_u)$$

and on the bottom surface

$$\bar{T}\, dS_l = \frac{\mu_0 I_r^2}{4\pi} d(\ln r_l) .$$

Since r_u is proportional to r_l, $d(\ln r_u) = d(\ln r_l)$, and the forces on the top of cylinder z are equal in magnitude and therefore cancel the forces on the cathode spot.

Because the radial forces acting on the cylinder cancel each other out, the only forces that affect the recoil force are the upward forces on the base of the cylinder that are not in the conducting channel. Thus the net force caused by the Lorentz forces is

$$\int_V (\bar{J} \times \bar{B})\, d\tau = \int_S \bar{\tau}\, dS_\ell$$

$$= \int_{r_c}^{r_s} \frac{\mu_o I^2}{4\pi}\, d(\ln r_\ell)$$

$$= \frac{\mu_o I^2}{4\pi} \ln \frac{r_s}{r_c} \,.$$

The pressure integral, $\int_V \nabla p\, d\tau$, can be put in the form $\oint_S p\, d\bar{S}$ which will allow us to calculate its contribution to the recoil force if an expression for p is known. Since the radial surfaces of the arc are at atmospheric pressure, the compressive forces at the anode and cathode are the only forces to be considered. The influence of the gas stream on these compressive forces will be neglected in the derivation, and this will be discussed later. In order to avoid using the assumption of uniform current density across the arc, a different method will be used to calculate $\oint_S p\, d\bar{S}$ than the method used to calculate p_{max}.

Starting with the equation of motion

$$\nabla p = \bar{J} \times \bar{B}$$

and neglecting the mass flow, the Maxwell equation, $\nabla \times \bar{B} = \mu_o \bar{J}$, will be used in determining ∇p.

$$\nabla p = \bar{J} \times \bar{B} = \frac{1}{\mu_o} (\nabla \times \bar{B}) \times \bar{B}$$

With $\nabla \times \bar{B} = \frac{1}{r} \frac{\partial (r B_\theta)}{\partial r} \hat{u}_z$ and $\bar{B} = B_\theta$

$$\nabla p = -\frac{1}{r \mu_o} \frac{\partial (r B_\theta)}{\partial r} B_\theta \hat{u}_r$$

Since ∇p is only in the r-direction,

$$\frac{dp}{dr} = -\frac{1}{r \mu_o} \frac{\partial (r B_\theta)}{\partial r} B_\theta$$

Integrating

$$\int_{p_{r=o}}^{p_r} dp = -\int_{r=o}^{r} \frac{1}{r \mu_o} \frac{\partial (r B_\theta)}{\partial r} B_\theta \, dr$$

Simplifying limits

$$p_r - p_{r=o} = -( )\big|_r + ( )\big|_{r=o}$$
$$p_{rs} - p_{r=o} = -( )\big|_{rs} + ( )\big|_{r=o}$$

or $$p_r - p_{rs} = -( )\big|_r + ( )\big|_{rs}$$

therefore,

$$p_r - p_{rs} = \int_r^{r_s} \frac{1}{r \mu_o} \frac{\partial (r B_\theta)}{\partial r} B_\theta \, dr$$

Let $p_r - p_{rs} = p$ gage.

The total compressive force of the surface is

$$\int p \, d\bar{s} = \int_0^{r_s} p \, 2\pi r \, dr = \frac{2\pi}{\mu_o} \int_0^{r_s} r \int_r^{r_s} \frac{1}{r} \frac{\partial (r B_\theta)}{\partial r} B_\theta \, dr dr .$$

Integrating by parts

$$\frac{2\pi}{\mu_0}\int_0^{r_s} r \int_r^{r_s} \frac{B_\theta}{r}\frac{\partial(rB_\theta)}{\partial r}\,dr\,dr =$$

$$\frac{2\pi}{\mu_0}\left[r^2\int_r^{r_s}\frac{B_\theta}{r}\frac{\partial(rB_\theta)}{\partial r}dr\right]\Bigg|_0^{r_s} - \frac{2\pi}{\mu_0}\int_0^{r_s} r\,d\left[r\left\{\int_r^{r_s}\frac{B_\theta}{r}\frac{\partial(rB_\theta)}{\partial r}dr\right\}\right] =$$

$$\left[r^2\int_r^{r_s}\frac{B_\theta}{r}\frac{\partial(rB_\theta)}{\partial r}dr\right]_0 = 0$$

$$-\frac{2\pi}{\mu_0}\int_0^{r_s} r B_\theta \frac{\partial(rB_\theta)}{\partial r}dr - \frac{2\pi}{\mu_0}\int_0^{r_s} r\int_r^{r_s}\frac{B_\theta}{r}\frac{\partial(rB_\theta)}{\partial r}dr\,dr$$

Adding terms

$$\int \rho\, d\bar{s} = -\frac{\pi}{\mu_0}\int_0^{r_s}(rB_\theta)\frac{\partial(rB_\theta)}{\partial r}dr$$

$$= -\frac{\pi}{\mu_0}\frac{(rB_\theta)^2}{2}\Bigg|_0^{r_s}$$

$$= -\frac{\pi}{2\mu_0} r_s^2 B_{\theta r_s}^2$$

Using the expression, $B_\theta = \frac{\mu_0}{r}\int_0^r J_z\, r\,dr$, derived previously, $\int \rho\, d\bar{s}$ can be put in the following form:

$$B_{\theta r_s} = \frac{\mu_0}{r_s 2\pi}\int_0^{r_s} 2\pi\, J_z\, r\,dr$$

With $$I = \int_0^{r_s} 2\pi J_z r dr$$

$$B_{\theta r_s} = \frac{\mu_0 I}{r_s 2\pi} ;$$

therefore,

$$\int \rho d\bar{s} = -\frac{\pi}{2\mu_0} r_s^2 \frac{\mu_0^2 I^2}{r_s^2 4\pi^2}$$

$$= -\frac{\mu_0 I^2}{8\pi}$$

With the compressive force $\int \rho d\bar{s}$ only dependent upon the total current, the net forces, $\oint_s \rho d\bar{s}$, from the cathode and anode areas on the arc will be zero.

With the pressure integral equal to zero, the only remaining force contributing to the recoil force is the Lorentz force.

$$F_c = \frac{\mu_0 I^2}{4\pi} \ln \frac{r_s}{r_c}$$

Maecker justifies the assumption of neglecting the stream in the pressure integral as follows: Since the stream coming out of the top surface of cylinder z (see figure above) is practically parallel to the axis, and the pressure gradient is radial, the stream should not influence the $\int_V \nabla p dT$. At the cathode surface, with the velocity on the axis equal to zero, the only effect the stream would have is to make the pressure fall off more rapidly in the radial direction. If this would halve the $\int \rho d\bar{s}$ making it equal to $\frac{\mu_0 I^2}{16\pi}$, this would only attribute to an error of about 20%, since the $\ln \frac{r_s}{r_c}$ in $\frac{\mu_0 I^2}{4\pi} \ln \frac{r_s}{r_c}$ is around 5/4.

APPENDIX B

TEMPERATURE OF A REFRACTORY CATHODE SPOT

One point that has been bothering us when studying the emission mechanism of refractory cathodes is the following: First, we assume that the emission mechanism is one of thermionic emission which would mean a current density of 10^3 a/cm^2. But with this low current density, it would take many seconds to heat up the cathode surface to a high enough temperature to produce this current density. Since we know from experiments that refractory cathode arcs occur in durations down to 13 μ sec., it seems that they could not be explained by heat conduction to the cathode.

This apparent contradiction can be understood if we look at some work done by Sigmond[64] with 30 nanosecond (n sec.) arcs. Although these discharges are called nanosecond arcs, they correspond to what we call sparks (duration less than 1 μ sec.).

Photographing the arc channel to find its diameter, Sigmond determined the current density to be greater than 10^6 a/cm^2. Sigmond also states that the voltage across the arc is less than 150 volts during the discharge, but that the voltage drops to 20-40 volts when the arc is extinguished. Applying one-dimensional heat conductivity theory, Sigmond calculates the time (t) needed to reach the boiling temperature of tungsten ($T_B \sim 6000\ ^oK$).

$$t = \frac{\pi \rho c k}{4} \left(\frac{T}{W/A}\right) = 3.6 \text{ nsec.} \qquad \text{for } W = 5 \text{ kw}, A = 3 \times 10^{-5} \text{ cm}^2$$

This calculation assumes that all the energy going into the arc is directed toward the cathode. Sigmond justifies this by stating that "the cathode electron-emission mechanism is certainly very inefficient

until a minimum cathode-gas sheath density and/or a minimum cathode spot temperature is established, resulting in a high cathode fall voltage, a high positive ion current distribution, and a correspondingly high cathode dissipation during this interval."

Thus Sigmond's calculation shows us that during the spark the cathode surface temperature can be raised to a high enough temperature to give appreciable thermionic emission. In fact, Sigmond does observe tungsten vapor after 3 nsec. which corresponds to the time needed to reach the boiling point. A word of caution must be given in believing Sigmond's exact values for voltage and current, because of the great difficulties in taking these measurements in nanoseconds. Apart from this admonition, Sigmond does give a good description of what would cause this high voltage.

Sigmond's work also gives us an explanation of the erosion found on the anode when using a refractory cathode. The erosion can be caused by the spark preceding the arc with the high current density (10^6 a/cm^2) observed by Sigmond. Along with the condensation of electrons on the anode which would heat it up, a shock wave is present (Somerville[54]) in a spark; therefore, we believe that with the close spacing encountered in EDM, the initial anode crater observed is caused by this high current density heating the surface and the shock wave.

APPENDIX C

FIGURES

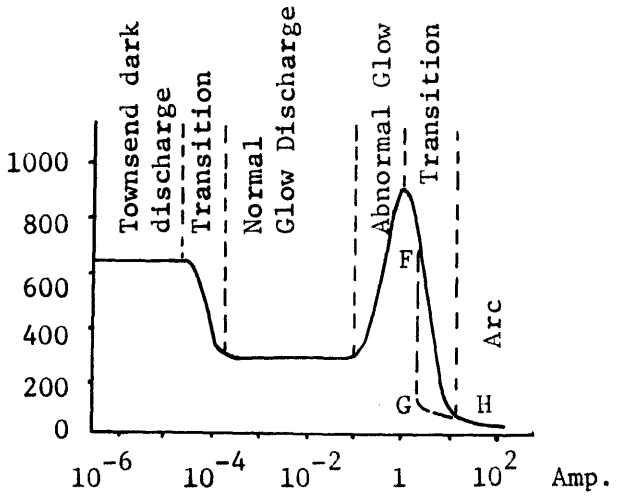

Fig. 1 Static Voltage-Current Diagram of a Discharge at Low Pressures; ∿ 1 mm Hg. (Somerville[8] p. 2)

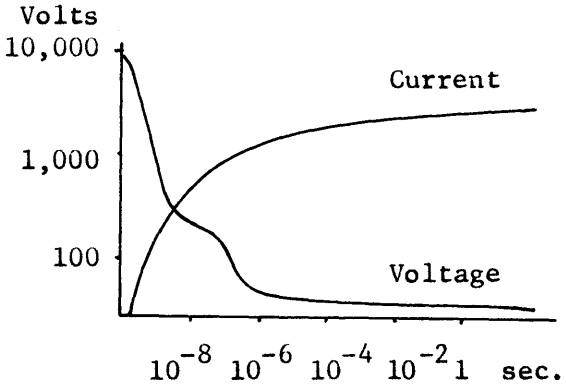

Fig. 2 Variation with Time of Current and Voltage between Two Electrodes in a Gas at ∿ 1 atm. Shortly after Breakdown has Taken Place. (Somerville[8] p. 4)

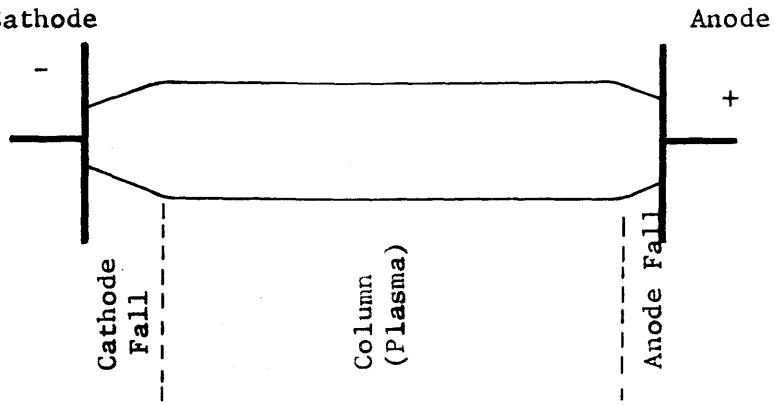

(a) Profile of Arc

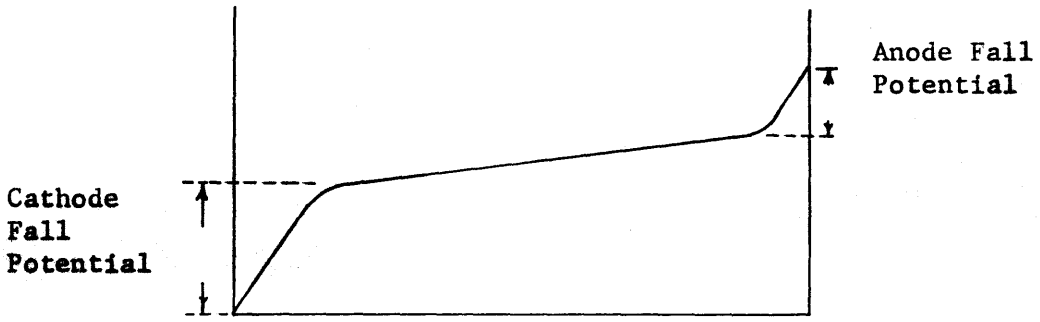

(b) Potential Across Gap

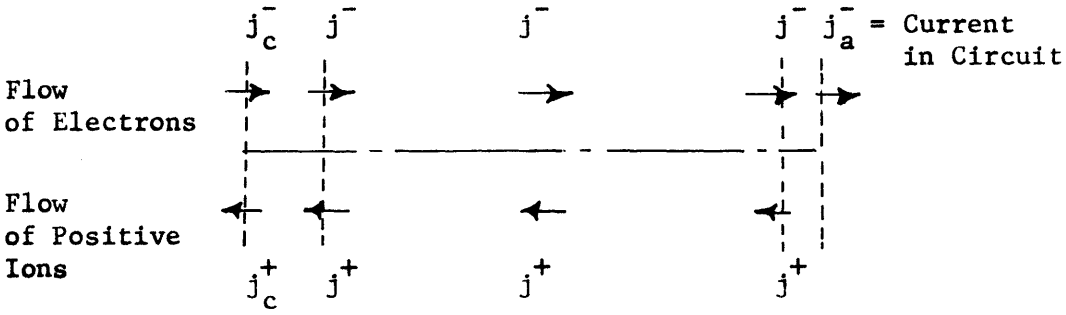

$j_c^+ \sim .10(j_c^+ + j_c^-)$ $\quad (j^- >> j^+)$ in Column

(c) Electron and Ion Current

Fig. 3 Arc Characteristics. (Somerville[8] p. 5 and p. 86)

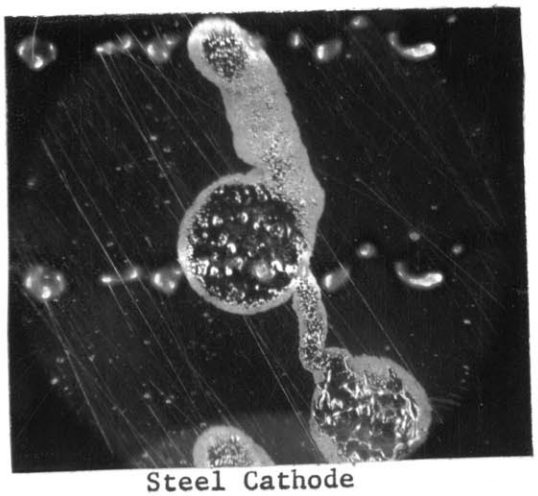

Steel Cathode

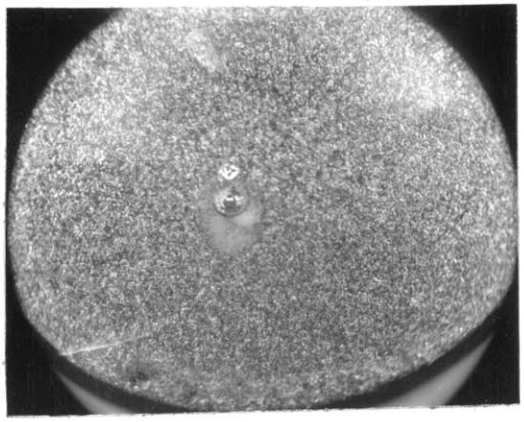

Cu Cathode

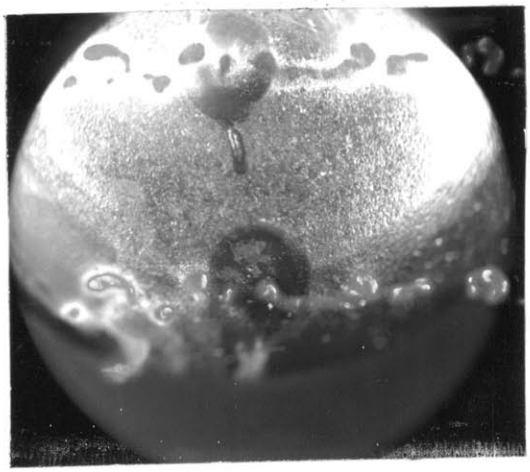

Cu Anode

(a) 50 amp, 0.007" Gap, 3200 μs

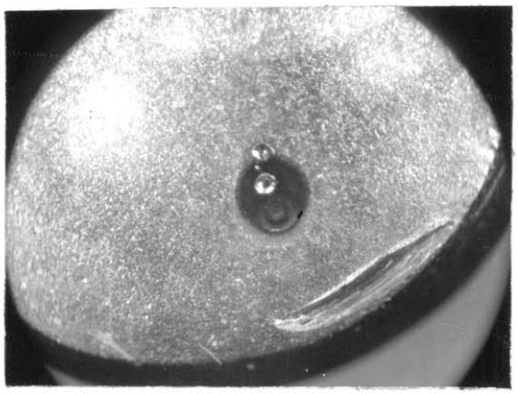

Cu Anode

(b) 60 amp, 0.001" Gap, 430 μs

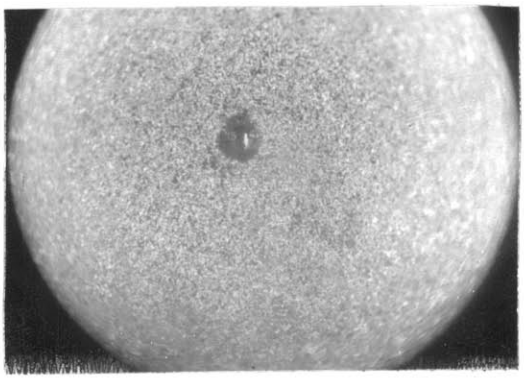

Cu Anode

(c) 50 amp, 0.005" Gap, 13 μs
using C Cathode

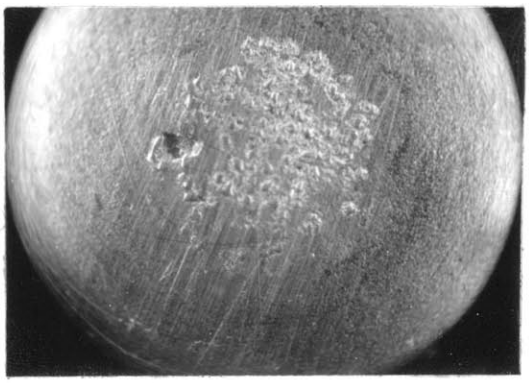

Cu Anode

(d) 50 amp, 0.005" Gap, ∿3 sec.
using C Cathode

Fig. 4 Photomicrographs (16X) of Discharges in Oil Using Single-Discharge Apparatus (Doret[3])

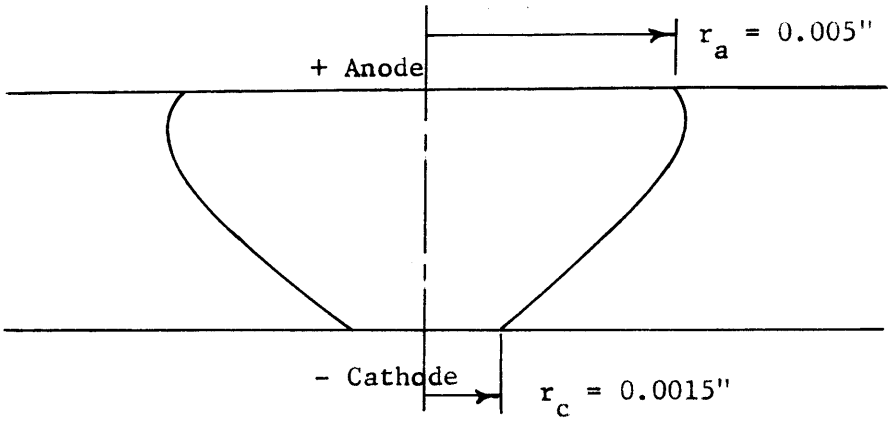

(a) (Gap = 0.005")

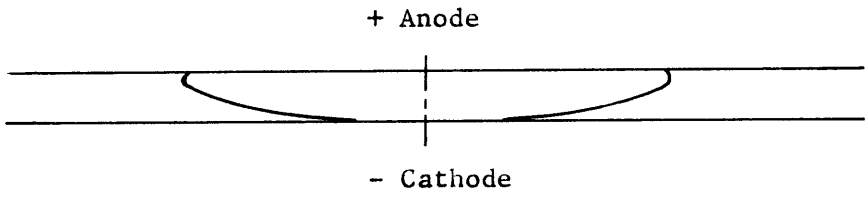

(b) (Gap = 0.001")

Fig. 5 Arc Profile for a 50 Amp Arc with $j_c = 1.1 \times 10^6$ a/cm^2, $j_a = 10^5$ a/cm^2

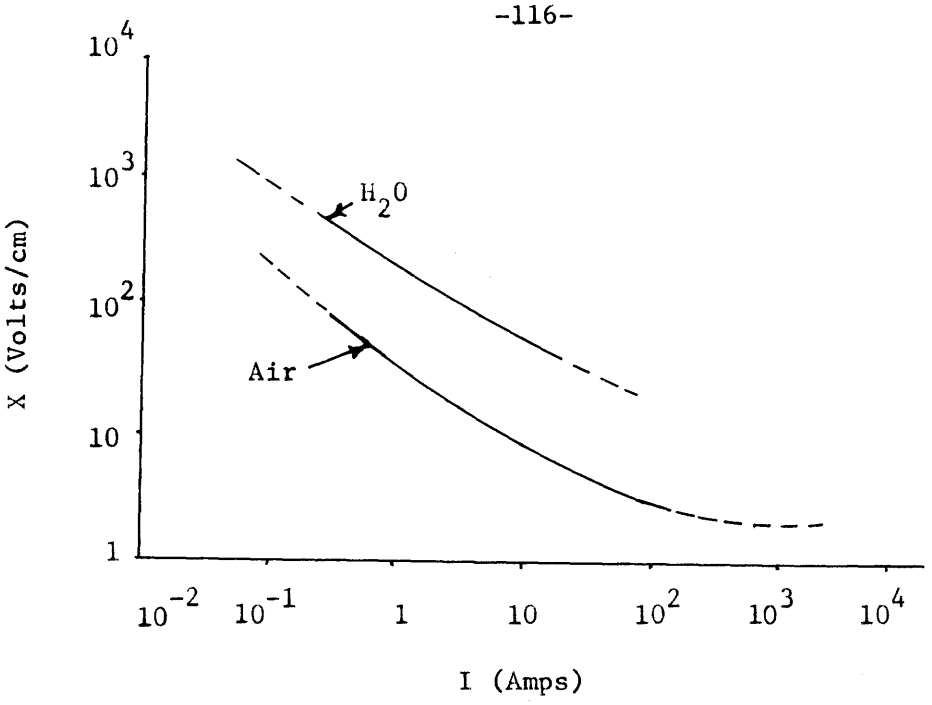

Fig. 6 Longitudinal Component of Electric Field (X) in a Positive Arc Column as a Function of the Current I at 1 Atmosphere (Von Engel[11] p. 262)

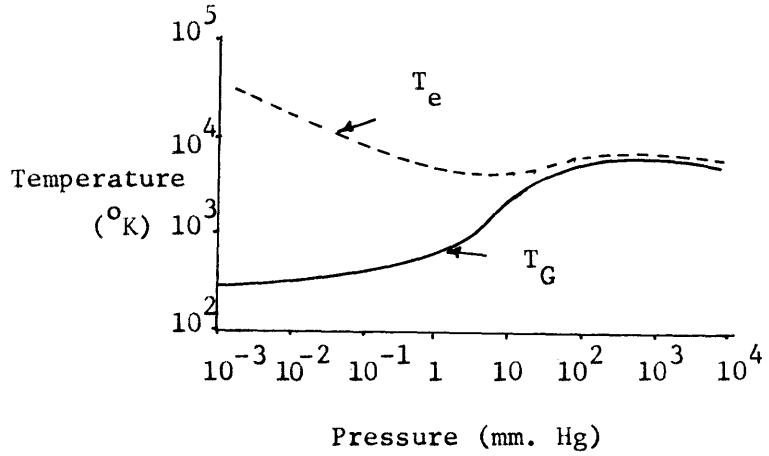

Fig. 7 Variation of Gas and Electron Temperature with Pressure in a Mercury Arc. (Somerville[8] p. 23)

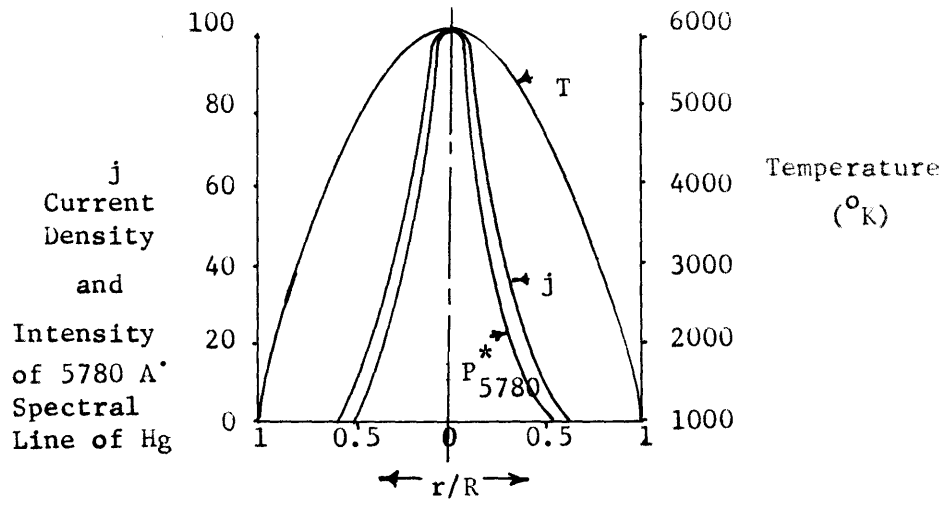

Fig. 8 Radial Variation of Temperature T, Current Density j, and Intensity P^*_{5780} of the 5780 A° Hg Spectral Lines Across an Arc Column in Hg Vapour at a Pressure ∿ 1 atm. (Somerville[8] p. 41)

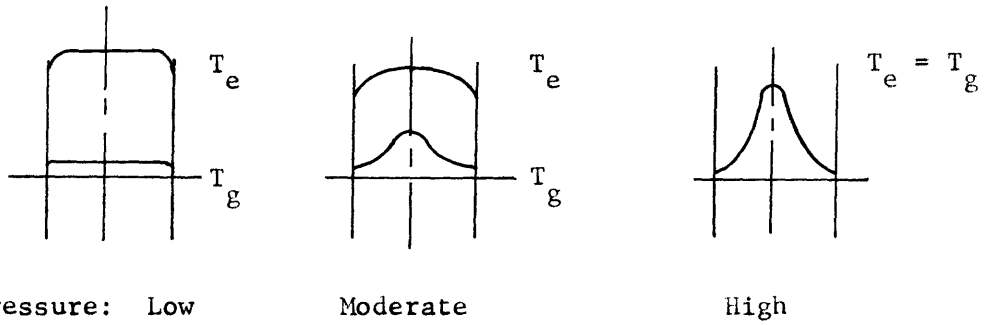

Fig. 9 Radial Distribution of Electron and Gas Temperature T_e and T_g at Various Pressures. (Von Engel[11] p. 265)

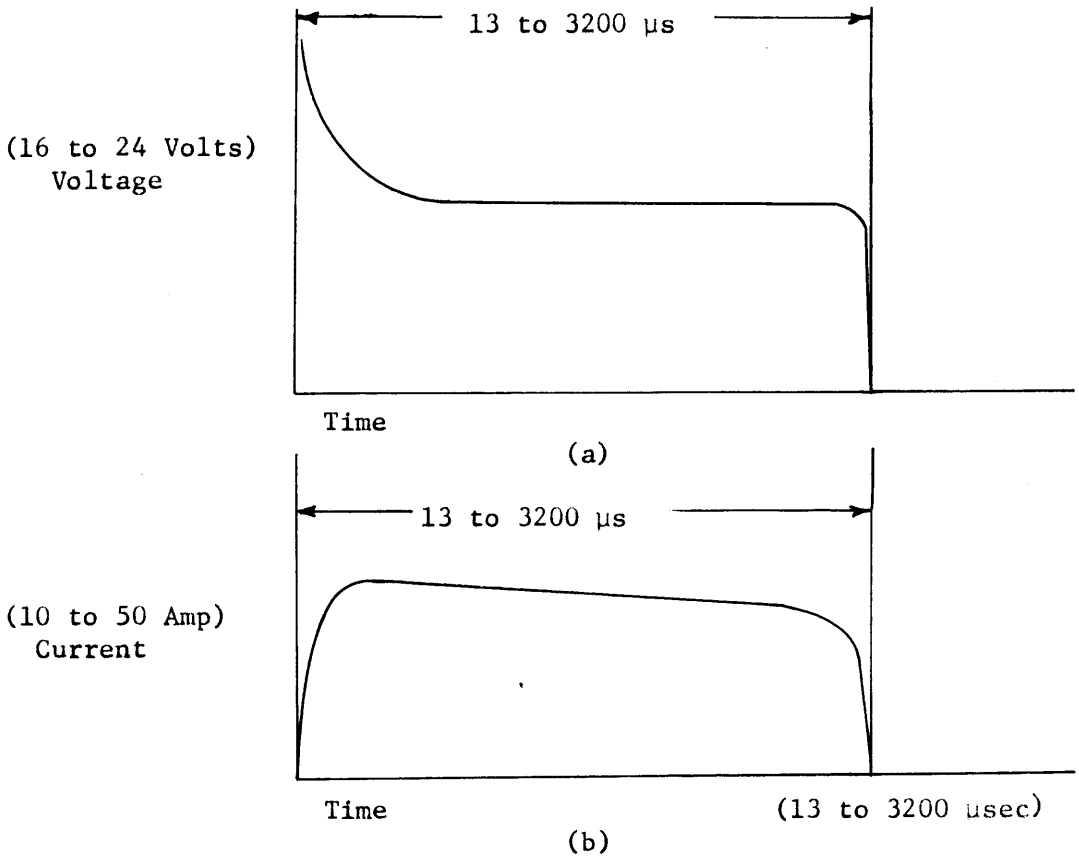

Fig. 10 Typical Voltage and Current Traces for Single Discharge Apparatus (Doret[3])